Chapter 1
Introduction to Dynamic Bifurcation Theory

1.1 Introduction

The change in the qualitative behavior of solutions as a control parameter (or control parameters) in a system is varied and is known as a *bifurcation*. When the solutions are restricted to neighborhoods of a given equilibrium, a bifurcation occurs often when the zero solution of the linearization of the system at the equilibrium changes its stability. To illustrate the basic concepts of bifurcation phenomena, we consider the following continuous dynamical system defined by the C^r ($r \geq 1$) vector field f: $\Lambda \times U \to \mathbb{R}^n$:

$$\dot{x} = f(\mu, x), \quad \mu \in \Lambda \subseteq \mathbb{R}^m, \quad x \in U \subseteq \mathbb{R}^n, \tag{1.1}$$

where U and Λ are open sets, x is the state variable, and μ is the (bifurcation) parameter.

Continuously varying μ may change the qualitative behavior of the solutions of (1.1). A value $\mu \in \Lambda$ for which such a change occurs is called a *bifurcation* (*critical*) *value*. The set of all bifurcation values is called the *bifurcation set* in the parameter space $\mathbb{R}^m$. We may use a bifurcation diagram to schematically show the considered solutions (equilibria/fixed points, closed orbits/periodic orbits, invariant tori) of a system as a function of a bifurcation parameter in the system. It is normal to represent stable solutions with solid lines and unstable solutions with dashed lines.

Local bifurcations are relevant to the birth or initiation of bifurcations when the bifurcation parameter is close to a bifurcation value. A local bifurcation from a given solution (an equilibrium, a periodic orbit, etc.) can normally be detected from a local stability analysis at the given solution. The global bifurcation thereby concerns the continuation of a local bifurcation when the bifurcation parameter is away from the bifurcation value.

The bifurcation phenomena is linked closely to the concepts of topological equivalence, structural stability, and genericity, which are described in the next section.

S. Guo and J. Wu, *Bifurcation Theory of Functional Differential Equations*,
Applied Mathematical Sciences 184, DOI 10.1007/978-1-4614-6992-6_1,

1.2 Topological Equivalence

In the study of dynamical systems, we are interested in not only specific solutions of a specific system, but also classification of solutions of a particular system and classification of systems according to general qualitative behaviors, that is, the number, position, and stability of equilibria, periodic orbits, and other isolated invariant sets.

In what follows, we will not distinguish a flow and a dynamical system. This means that we consider a continuous mapping $\Phi\colon \mathbb{R}\times U\to U$ over an open set $U\subseteq\mathbb{R}^n$ such that $\Phi(0,x)=x$ and $\Phi(t,\Phi(s,x))=\Phi(t+s,x)$ for t, $s\in\mathbb{R}$, and $x\in U$. Sometimes, we write it as $\Phi^t:=\Phi(t,\cdot)\colon U\to U$ for $t\in\mathbb{R}$.

We consider two dynamical systems to be (locally) equivalent if their (local) phase portraits are similar in a qualitative sense, that is, if they can be locally transformed into each other through a continuous transformation. More precisely, we introduce the following definition.

Definition 1.1. A dynamical system Φ in $\mathbb{R}^n$ is said to be *topologically equivalent* in a region $U\subset\mathbb{R}^n$ to a dynamical system Ψ in a region $V\subset\mathbb{R}^n$ if there exists a homeomorphism $h\colon U\to V$ that maps the orbits of Φ in U onto the orbits of Ψ in V, preserving the direction of time.

A homeomorphism is an invertible map such that both the map and its inverse are continuous. A homomorphism is called a diffeomorphism if it is C^1-smooth and its inverse is also C^1-smooth. The definition of topological equivalence can be generalized to cover more general cases in which the state space is a complete metric or, in particular, a Banach space. The definition also remains meaningful when the state space is a smooth finite-dimensional manifold in $\mathbb{R}^n$, for example, a two-dimensional torus $\mathbb{T}^2$ or sphere $\mathbb{S}^2$. The phase portraits of topologically equivalent systems are often said to be topologically equivalent.

Example 1.1. Consider the flows Φ^t and Ψ^t associated with the differential equations

$$\dot{x}=-x \quad\text{and}\quad \dot{y}=-3y,$$

respectively. The homeomorphism $h\colon\mathbb{R}\to\mathbb{R}$ given by $h(x)=x^3$ for $x\in\mathbb{R}$ maps the orbits of Φ onto those of Ψ.

Definition 1.2. Two flows Φ^t (on U) and Ψ^t (on V) are called *topologically conjugate* if there exists a homeomorphism $h\colon U\to V$ such that

$$\Psi^t=h\circ\Phi^t\circ h^{-1}\quad\text{for}\quad t\in\mathbb{R}.$$

We also use the term *smoothly conjugate* (or *diffeomorphic*) if the involved homeomorphism is a diffeomorphism and the flows are smooth.

For example, for a continuous-time system

$$\dot{x}=f(x),\quad x\in\mathbb{R}^n, \tag{1.2}$$

if h is a diffeomorphism from $\mathbb{R}^n$ to $\mathbb{R}^n$, and $x = h(y)$, then the system

$$\dot{y} = g(y), \quad y \in \mathbb{R}^n \tag{1.3}$$

with $g(y) = [Dh(y)]^{-1} f(h(y))$ for all $y \in \mathbb{R}^n$ is smoothly equivalent (or diffeomorphic) to system (1.2). In fact, denoting by $\Phi^t(x)$ the flow associated with system (1.2), and letting $\Psi^t(y) = h^{-1}(\Phi^t(h(y)))$, we have

$$Dh(\Psi^t(y))\frac{\mathrm{d}}{\mathrm{d}t}\Psi^t(y) = f(\Phi^t(h(y))),$$

and so

$$\frac{\mathrm{d}}{\mathrm{d}t}\Psi^t(y) = [Dh(\Psi^t(y))]^{-1} f(\Phi^t(h(y))) = g(\Psi^t(y)),$$

which implies that $\Psi^t(y)$ is the flow associated with system (1.3). Therefore, systems (1.2) and (1.3) are smoothly equivalent (or diffeomorphic).

In what follows, if the degree of smoothness of h is of interest, we also use the term C^k-equivalent or C^k-diffeomorphic.

Two diffeomorphic systems are practically identical and can be viewed as the same system written using different coordinates. Two diffeomorphic systems have similar qualitative behaviors. For such systems, the eigenvalues of corresponding equilibria are the same: Let x_0 and $y_0 = h(x_0)$ be such equilibria and let $A(x_0)$ and $B(y_0)$ denote corresponding Jacobian matrices. Then we have

$$A(x_0) = M^{-1}(x_0)B(y_0)M(x_0),$$

where $M(x) = Dh(x)$. Therefore, the characteristic polynomials for the matrices $A(x_0)$ and $B(y_0)$ coincide.

It is easy to construct nondiffeomorphic but topologically equivalent flows. To see this, consider a smooth scalar position function $\mu\colon \mathbb{R}^n \to (0,\infty)$ and assume that the right-hand sides of (1.2) and (1.3) are related by

$$f(x) = \mu(x)g(x) \quad \text{for} \quad x \in \mathbb{R}^n. \tag{1.4}$$

Then systems (1.2) and (1.3) are topologically equivalent since their orbits are identical, and it is the velocity of the motion that makes them different. Thus, the homeomorphism h in Definition 1.1 is the identity map $h(x) = x$. In other words, these two systems are distinguished only by the time parameterization along the orbits. We say that two systems (1.2) and (1.3) satisfying (1.4) for a smooth positive function μ are *orbitally equivalent*. Usually, two orbitally equivalent systems can be nondiffeomorphic, having cycles that look like the same closed curve in the phase space but different periods. For example, the system

$$\dot{r} = r(1-r), \quad \dot{\theta} = 1$$

and the system

$$\dot{\rho} = 2\rho(1-\rho), \quad \dot{\varphi} = 2$$

in $\mathbb{R}^2$ using polar coordinates are topologically equivalent, but not topologically conjugate, because their periodic orbits $r = 1$ and $\rho = 1$ have periods 2π and π, respectively.

Let x_0 be an equilibrium of the system (1.2), that is, $f(x_0) = 0$, and let A denote the Jacobian matrix $Df(x)$ evaluated at $x = x_0$. Let n_-, n_0, and n_+ be the numbers of eigenvalues of A (counting multiplicities) with negative, zero, and positive real part, respectively. Recall that an equilibrium is called *hyperbolic* if $n_0 = 0$, that is, if A has no purely imaginary eigenvalues. A hyperbolic equilibrium is called a *hyperbolic saddle* if $n_- n_+ \neq 0$.

Topological equivalence of linear systems is generally easy to determine. If the linearized flow near an equilibrium is asymptotically stable, then the equilibrium is asymptotically stable. Moreover, two asymptotically stable n-dimensional linear flows are topologically equivalent.

Example 1.2. Consider two linear planar systems:

$$\dot{x} = -x, \quad \dot{y} = -y, \tag{1.5}$$

and

$$\dot{x} = -x - y, \quad \dot{y} = x - y. \tag{1.6}$$

Clearly, the origin is a stable equilibrium in both systems. All other trajectories of (1.5) are straight lines, while those of (1.6) are spirals. The equilibrium of the first system is a node, while in the second systems it is a focus. These two systems are neither orbitally nor smoothly equivalent. However, they are topologically equivalent.

We can further claim that *near a hyperbolic equilibrium p, the system behaves essentially like the linearized one*. In other words, Φ^t is topologically equivalent to $e^{Df(p)t}$ in a sufficiently small neighborhood of a hyperbolic equilibrium p (Grobman–Hartman theorem). See Grobman [123], Hartman [161, 162], Hirsch [163], Hale and Kocak [152] for details. As a result, determining topological equivalence near hyperbolic equilibria boils down to counting the dimensions of the local stable and unstable subspaces (manifolds).

Theorem 1.1. *Two systems of differential equations with hyperbolic equilibria are topologically equivalent near these equilibria if and only if their linearizations have the same number n_+ of eigenvalues with positive real parts and the same number n_- of eigenvalues with negative real parts.*

1.3 Structural Stability

There are dynamical systems whose phase portrait (in some domain) does not change qualitatively under all sufficiently small perturbations. For example, suppose that (1.1) has an equilibrium x_0 when $\mu = \mu_0$, that is,

$$f(\mu_0, x_0) = 0. \tag{1.7}$$

It is natural to ask about the stability of this equilibrium and how the stability or instability is affected as μ is varied. Thus, we first linearize (1.1) at (μ_0, x_0) to get

$$\dot{x} = D_x f(\mu_0, x_0)x, \quad x \in \mathbb{R}^n. \tag{1.8}$$

If the eigenvalues of the linearized matrix $D_x f(\mu_0, x_0)$ are all nonzero, then the linearized matrix is invertible, and by an application of the implicit function theorem, there is a curve $\mu \to \beta(\mu)$ in $\mathbb{R}^n$ such that $\beta(\mu_0) = x_0$ and $f(\mu, \beta(\mu)) \equiv 0$ for all sufficiently small $|\mu - \mu_0|$. In other words, for each μ in the domain of β, the point $\beta(\mu) \in \mathbb{R}^n$ corresponds to an equilibrium point for the member of the family (1.1) at the parameter value μ.

If the equilibrium x_0 is hyperbolic, that is, none of eigenvalues of the linearized matrix $D_x f(\mu_0, x_0)$ lie on the imaginary axis, then the linearized matrix of (1.1) at $(\mu, \beta(\mu))$ is $D_x f(\mu, \beta(\mu))$ it depends smoothly on μ and coincides with $D_x f(\mu_0, x_0)$ at $\mu = \mu_0$. Recall that if $D_x f(\mu_0, x_0)$ has no eigenvalues on the imaginary axis, then neither does $D_x f(\mu, \beta(\mu))$ for each μ in a sufficiently small neighborhood of μ_0. In other words, $\beta(\mu)$ is a hyperbolic equilibrium of (1.1) for all μ in a sufficiently small neighborhood of μ_0. Moreover, the numbers n_+ and n_- of the positive and negative eigenvalues of $D_x f(\mu, \beta(\mu))$ are fixed for these values of μ. In view of Theorem 1.1, system (1.1) is locally topologically equivalent to $\dot{x} = f(\mu_0, x)$ near the equilibria. This means that *a hyperbolic equilibrium is structurally stable under smooth perturbations*.

Inspired by the above property, we now can define a structurally stable system, which means that every sufficiently close system is topologically equivalent to the structurally stable one.

Definition 1.3. A flow Φ is said to be *structurally stable* in a region $D \subset \mathbb{R}^n$ if for every flow Ψ that is sufficiently C^1-close to Φ, there exist regions U and V with $D \subset U$ such that Ψ is topologically equivalent in V to Φ in U.

The following theorem results from the previous discussion.

Theorem 1.2. *A flow with a hyperbolic equilibrium is structurally stable in a neighborhood of the equilibrium.*

In Definition 1.3, we require the C^1 metric, instead of C^0, because two C^0 curves may be arbitrarily close to each other but have different numbers of equilibria. Moreover, it would be nice to show that structurally stable systems are generic. The following classical theorem gives necessary and sufficient conditions for a continuous-time system in a plane to be structurally stable.

Theorem 1.3 (Andronov and Pontryagin [16]). *A smooth dynamical system*

$$\dot{x} = f(x), \quad x \in \mathbb{R}^2,$$

is structurally stable in a region $D_0 \subset \mathbb{R}^2$ if and only if

(i) The number of equilibria and periodic orbits is finite and each is hyperbolic;
(ii) There are no orbits connecting saddle points.

Furthermore, for two-dimensional vector fields on compact manifolds, we have the following result due to Peixoto [244].

Theorem 1.4 (Peixoto's theorem [244]). *Let $\mathscr{D}$ be a compact two-dimensional manifold without boundary and let $\mathscr{X}^k(\mathscr{D})$ denote the C^k ($k \geq 1$) vector fields defined on $\mathscr{D}$. Then $f \in \mathscr{X}^k(\mathscr{D})$ is structurally stable on $\mathscr{D}$ if and only if*

(i) The number of equilibria and periodic orbits is finite and each is hyperbolic;
(ii) There are no orbits connecting saddle points;
(iii) The nonwandering set consists of equilibria and periodic orbits.

Moreover, if D is orientable, then the set of such vector fields is open and dense in $\mathscr{X}^k(\mathscr{D})$.

This theorem is useful because it spells out precise conditions for structural stability on the dynamics of a vector field on a compact two-manifold without boundary under which it is structurally stable. Unfortunately, we do not have a similar theorem in higher dimensions. This is in part due to the presence of complicated recurrent motions (e.g., the Smale horseshoe). In light of this theorem, it appears to be practically convenient to ignore more structurally unstable vector fields defined on a compact two-dimensional manifold without boundary, because an arbitrarily small perturbation will usually turn a structurally unstable vector field into a structurally stable one. However, as we shall see, if this vector field depends on a parameter, more complicated dynamics will take place.

1.4 Codimension-One Bifurcations of Equilibria

Let x_0 be a hyperbolic equilibrium point of (1.1) for $\mu = \mu_0$. As we have seen in the previous section, under a small parameter variation, the equilibrium moves slightly but remains hyperbolic. Therefore, we can vary the parameter further and control the equilibrium. It is clear that there are, generically, only two ways in which the hyperbolicity condition can be violated. Either a simple real eigenvalue approaches zero, or a pair of simple complex eigenvalues reaches the imaginary axis for some values of the parameter.

If the equilibrium x_0 of (1.1) is not hyperbolic, that is, $D_x f(\mu_0, x_0)$ has some eigenvalues on the imaginary axis, then the topology of the local phase portrait of the corresponding differential equation (1.1) at this equilibrium point may change under perturbation, that is, a bifurcation occurs. For example, equilibria can be created or destroyed, and time-dependent behavior such as periodic, quasiperiodic, homoclinic, heteroclinic, or even chaotic dynamics can be created. Moreover, the more eigenvalues on the imaginary axis, the more complicated the dynamics will be.

For equilibria of flows, a (generic) codimension-one bifurcation means that the crossing of the stability region (the imaginary axis) is taking place with either one eigenvalue of the linear part going through 0 or one pair of complex conjugate eigenvalues crossing the imaginary axis. This section will be devoted essentially to the

proof that a nonhyperbolic equilibrium satisfying one of these two conditions is structurally unstable and to the analysis of the corresponding bifurcations of the local phase portrait under variation of the parameter.

Definition 1.4. The bifurcation associated with the appearance of eigenvalue 0 is called a *fold* (or *tangent*) bifurcation.

This bifurcation is also associated with a lot of other names, including limit point and turning point.

Definition 1.5. The bifurcation corresponding to the presence of a pair of complex purely imaginary eigenvalues is called a *Hopf* (or *Andronov–Hopf*, or *Poincaré–Andronov–Hopf*) bifurcation.

As pointed out repeatedly by Arnold [19], examples of Hopf bifurcation can be found in the work of Poincaré [248]. The first specific study and formulation of a theorem in this area was due to Andronov [14]. However, the work of Poincaré and Andronov was concerned with two-dimensional vector fields. The existence of such a bifurcation was found in the context of general n-dimensional ordinary differential equations (ODEs) by Hopf [167] in 1942. This was before the discovery of the center manifold theorem. For these reasons, we usually refer to this kind of bifurcation as a Poincaré–Andronov–Hopf bifurcation.

In the 1970s, Hsu and Kazarinoff [169], Poore [250], Marsden and McCracken [217], and others discussed in their works the computation of important features of the Hopf bifurcation, especially the direction of bifurcation and dynamical aspects (stability, attractiveness, etc.), both from theoretical and numerical standpoints. A very important new achievement was the proof by Alexander and Yorke [10] of what is known as the global Hopf bifurcation theorem, which, roughly speaking, describes the global continuation of the local branch. The theory was also extended to allow further degeneracies (more than two eigenvalues crossing the imaginary axis, or multiplicity higher than one, etc.), leading notably to the development of the generalized Hopf bifurcation theory (Bernfeld et al. [31, 32], Negrini and Salvadori [228]).

Now, if these phenomena were taking place in a linear system, then there would be just a low-dimensional (1 or 2, respectively) invariant subspace to be affected by the bifurcations. In what follows, we first study these bifurcations in systems of smallest possible dimension for the bifurcations to take place. Here, the effort will be to obtain expressions for these systems that are as simple as possible while still capturing the bifurcations of interest, and at the same time to show that other systems undergoing the same bifurcation are locally topologically equivalent to these simple ones. In subsequent chapters, we shall see that center manifold reduction can transform the bifurcation problem in general functional differential equations (of course, general n-dimensional ODEs) into that of ordinary differential equations on a one- or two-dimensional invariant manifold. Therefore, this part of study is basic and crucial for discussing bifurcations in general functional differential equations (see Chap. 7).

1.4.1 Fold Bifurcation

Consider the following one-parameter scalar ODE:

$$\dot{x} = f(\mu, x), \quad x,\ \mu \in \mathbb{R}, \tag{1.9}$$

where $f(0,0) = 0$. That is, (1.9) has an equilibrium $x_0 = 0$ when $\mu = \mu_0 = 0$. The condition ensuring a fold bifurcation of (1.9) is that $f_x(0,0) = 0$. Usually, we may encounter three situations, as discussed in this section.

Example 1.3. Consider the family of differential equations

$$\dot{x} = \mu - x^2, \quad x, \mu \in \mathbb{R}.$$

We see that $\mu = 0$ is the bifurcation value. In particular, if $\mu > 0$, then there are two equilibria: an unstable equilibrium $-\sqrt{\mu}$ and a stable one $\sqrt{\mu}$. At the bifurcation value $\mu = 0$, there is only one equilibrium, which is not hyperbolic. If $\mu < 0$, there are no equilibria. The bifurcation diagram is the parabola $\mu = x^2$ labeled as in Fig. 1.1. Notice that the parameter μ is assigned to the horizontal axis, while the stable equilibria are drawn in solid lines and the unstable equilibria in dashed lines.

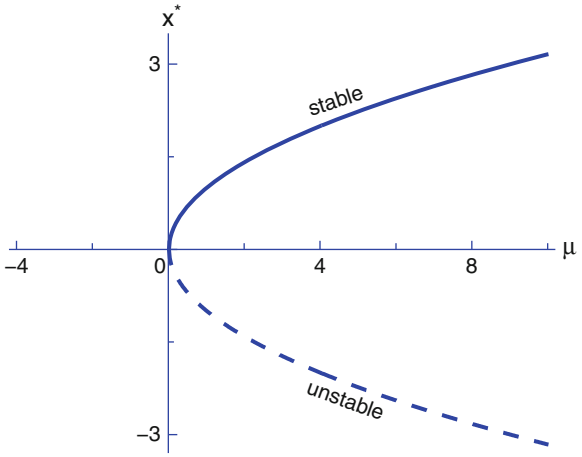

Fig. 1.1 Bifurcation diagram of a saddle-node bifurcation

The type of bifurcation described in Example 1.3—on one side of a parameter value there are no equilibria, and on the other side there are two equilibria—is referred to as a *saddle-node bifurcation*. The next theorem lists sufficient conditions for a saddle-node bifurcation to occur at $(\mu, x) = (0,0)$ in the scalar system (1.9). A more general theorem on saddle-node bifurcation will be formulated and proved later for general delay differential equations.

Theorem 1.5. *Suppose f in (1.9) is sufficiently smooth and satisfies*

$$f(0,0)=0, \quad f_x(0,0)=0, \quad f_\mu(0,0)f_{xx}(0,0)\neq 0. \tag{1.10}$$

Then there are smooth invertible local changes of coordinate and parameter that transform the system (1.9) into the following normal form:

$$\dot{y}=\gamma \pm y^2+O(|y|^3). \tag{1.11}$$

Therefore, if $f_\mu(0,0)f_{xx}(0,0)<0$ (respectively, >0), then near the origin, only two equilibria exist for $\mu>0$ (respectively, <0), only one equilibrium $x=0$ exists for $\mu=0$, and no equilibria exist for $\mu<0$ (respectively, >0). In the case that two equilibria exist, one is asymptotically stable and the other is unstable.

Proof. Expanding f with respect to x around $\mu=0$ yields

$$f(\mu,x)=f_0(\mu)+f_1(\mu)x+f_2(\mu)x^2+O(x^3),$$

where

$$f_j(\mu)=\frac{1}{j!}\frac{\partial^j f}{\partial x^j}(\mu,0), \quad j=0,1,2,\ldots.$$

Obviously, $f_0(0)=f(0,0)=0$ and $f_1(0)=f_x(0,0)=0$. Set $\xi=x+\delta$, where δ is a constant independent of t. Then (1.9) can be transformed into

$$\begin{aligned}\dot{\xi} &= f_0(\mu)-f_1(\mu)\delta+f_2(\mu)\delta^2+O(\delta^3)\\ &\quad +[f_1(\mu)-2f_2(\mu)\delta+O(\delta^2)]\xi+[f_2(\mu)+O(\delta)]\xi^2+O(\xi^3).\end{aligned} \tag{1.12}$$

Noting that $f_1(0)=0$ and $f_2(0)=\frac{1}{2}f_{xx}(0,0)\neq 0$, and using the implicit function theorem, we can find $\delta(\mu)$ for small μ such that $f_1(\mu)-2f_2(\mu)\delta+O(\delta^2)=0$. This gives

$$\delta(\mu)=\frac{f_{\mu x}(0,0)}{f_{xx}(0,0)}\mu+O(\mu^2).$$

Using this $\delta(\mu)$, we have

$$\dot{\xi}=\beta(\mu)+[f_2(\mu)+O(\mu)]\xi^2+O(\xi^3), \tag{1.13}$$

where $\beta(\mu)=f_0'(0)\mu+O(\mu^2)$. Recall that $f_0'(0)=f_\mu(0,0)\neq 0$. Then the function β is invertible near the origin. Hence, we can obtain $\mu(\beta)$ with $\mu(0)=0$. Thus, (1.13) can be changed into the form

$$\dot{\xi}=\beta\pm c(\beta)\xi^2+O(\xi^3),$$

where the sign is that of $f_{xx}(0,0)$ and c is a smooth positive function. Take $y=c(\beta)\xi$ and $\gamma=c(\beta)\beta$. Then we obtain (1.11), which is obviously topologically equivalent to $\dot{y}=\gamma\pm y^2$. The rest of the proof follows from Example 1.3. □

Remark 1.1. In the study of bifurcations, we usually have bifurcation conditions and genericity conditions (nondegeneracy conditions). For the saddle-node bifurcation

of (1.9), the bifurcation conditions are $f(0,0)=0$ and $f_x(0,0)=0$, and the genericity conditions are $f_\mu(0,0)=0$ and $f_{xx}(0,0)=0$. The bifurcation conditions will be used to numerically search for bifurcation points, while the genericity conditions will be used to verify whether a bifurcation point is really of the type we are looking for, i.e., to guarantee that locally, nothing more complicated can occur.

1.4.2 Poincaré–Andronov–Hopf Bifurcation

We start with a simple example in which a pair of simple complex conjugate eigenvalues cross the imaginary axis.

Example 1.4. Consider the following planar system:

$$\begin{aligned} \dot{x} &= \mu x - y - x(x^2+y^2), \\ \dot{y} &= x + \mu y - y(x^2+y^2), \end{aligned} \tag{1.14}$$

where $x,y,\mu \in \mathbb{R}$. Using the complex and polar coordinates $z = x+\mathrm{i}y = r\mathrm{e}^{\mathrm{i}\theta}$, system (1.14) takes the forms

$$\dot{z} = (\mu+\mathrm{i})z - z|z|^2$$

and

$$\dot{r} = r(\mu - r^2), \quad \dot{\theta} = 1,$$

which can be solved for (r,θ):

$$\begin{aligned} r &= \begin{cases} \sqrt{\mu(1+C\mathrm{e}^{-2\mu t})^{-1}}, & \mu \neq 0, \\ \sqrt{(2t+C)^{-1}}, & \mu = 0, \end{cases} \\ \theta &= t - t_0, \end{aligned} \tag{1.15}$$

where C and t_0 are determined by the initial condition. Variations of the phase portrait of system (1.14) as μ passes through zero can be easily analyzed using the polar form (1.15), since the equations for r and θ are uncoupled. We can see that system (1.14) always has a unique equilibrium at the origin, which is a stable focus for $\mu<0$ and an unstable focus for $\mu>0$. This equilibrium is surrounded for $\mu>0$ by an isolated closed orbit (limit cycle) that is unique and stable. This bifurcation is *supercritical* because the closed orbit (limit cycle) appears after the bifurcation.

The bifurcation diagram for periodic solutions of (1.14) is simply a plot of the solutions of $\mu = r^2$ in the (μ,r)-plane together with the line $r=0$ (see Fig. 1.2). As usual, stable periodic orbits are indicated by solid curves, and unstable ones with dashed curves.

Similarly, the system

$$\begin{aligned} \dot{x} &= \mu x - y + x(x^2+y^2), \\ \dot{y} &= x + \mu y + y(x^2+y^2), \end{aligned} \tag{1.16}$$

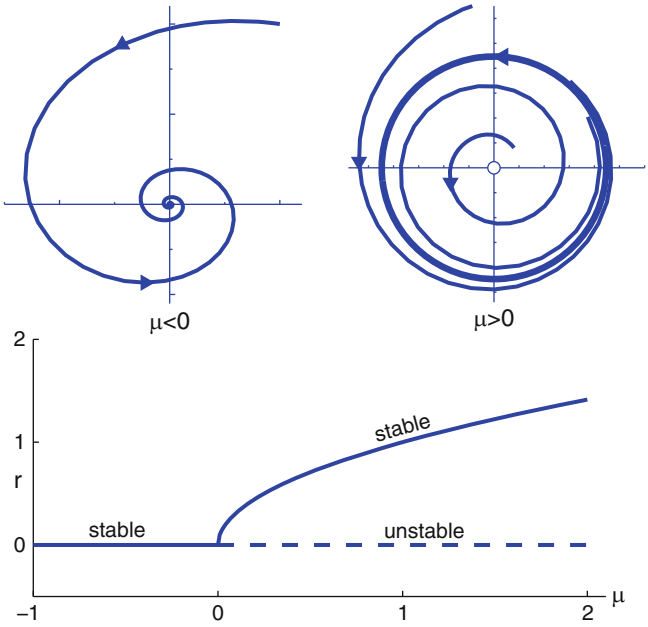

Fig. 1.2 A supercritical Hopf bifurcation

can be rewritten as

$$\dot{z} = (\mu + \mathrm{i})z + z|z|^2$$

or

$$\dot{r} = r(\mu + r^2), \quad \dot{\theta} = 1.$$

This has an unstable periodic solution (limit cycle) for $\mu < 0$. Hence this bifurcation is *subcritical*.

As described in Example 1.4, in a Poincaré–Andronov–Hopf bifurcation, an equilibrium of a system loses stability as a pair of complex conjugate eigenvalues of the linearization around the equilibrium cross the imaginary axis of the complex plane. Under reasonably generic assumptions about the dynamical system, we can expect a small-amplitude limit cycle branching from the fixed point. Either the limit cycle is orbitally stable and the bifurcation is supercritical, or the limit cycle is unstable and the bifurcation is subcritical.

The next theorem lists sufficient conditions for a Poincaré–Andronov–Hopf bifurcation to occur in a planar system.

Theorem 1.6 (Hassard and Wan [159]). *Consider the following system:*

$$\begin{bmatrix} \dot{x} \\ \dot{y} \end{bmatrix} = \begin{bmatrix} \mu & \omega \\ -\omega & \mu \end{bmatrix} \begin{bmatrix} x \\ y \end{bmatrix} + \begin{bmatrix} f^1(x,y) \\ f^2(x,y) \end{bmatrix}, \tag{1.17}$$

where $\omega > 0$ and f^j is three times differentiable, satisfying $f^j_x(0,0) = f^j_y(0,0) = 0$, $j = 1,2$. Then there exists a branch of periodic solutions of (1.17) bifurcating from the trivial solution $x = 0$, and the Poincaré–Andronov–Hopf bifurcation is supercritical (subcritical), i.e., bifurcating periodic solutions exist for $\mu > 0$ (respectively, < 0) if $\Upsilon < 0$ (respectively, > 0), where

$$\Upsilon = f^1_{xxx} + f^1_{xyy} + f^2_{xxy} + f^2_{yyy} + \frac{1}{\omega}[f^1_{xy}(f^1_{xx} + f^1_{yy}) - f^2_{xy}(f^2_{xx} + f^2_{yy}) - f^1_{xx}f^2_{xx} + f^1_{yy}f^2_{yy}].$$

More generally, in order to investigate Poincaré–Andronov–Hopf bifurcations in high-dimensional ODEs, even in infinite-dimensional ODEs generated by partial differential equations (PDEs) and functional differential equations (FDEs), we may employ center manifold reduction and normal form theory to obtain the following system:

$$\dot{z} = \lambda(\mu)z + C(\mu)z|z|^2 + O(|z|^5), \quad (\mu, z) \in \mathbb{R} \times \mathbb{C}, \tag{1.18}$$

where $\lambda(0) = \mathrm{i}\omega$ and $\omega > 0$. Detailed analysis can be found in Sects. 3.4.1, 4.3.1, and 7.3.2. Also see [54, 55, 74, 152, 200, 257, 282, 302] for more background on Poincaré-Andronov-Hopf bifurcation.

Definition 1.6. The first Lyapunov coefficient of a Hopf bifurcation is defined by $l_1(0) = \mathrm{Re}\{C(0)\}/\omega$.

As stated in Lemma 3.7 of Kuznetsov [200], if $\mathrm{Re}\{\lambda'(0)\}\mathrm{Re}\{C(0)\} \neq 0$, then (1.18) can be transformed by a parameter-dependent linear coordinate transformation, a time rescaling, and a nonlinear-time reparameterization into an equation of the form

$$\dot{z} = (\beta + \mathrm{i})z + sz|z|^2 + O(|z|^5), \quad (\mu, z) \in \mathbb{R} \times \mathbb{C}, \tag{1.19}$$

where $s = \mathrm{sgnRe}\{C(0)\} = \mathrm{sgn}l_1(0)$ and β is the new parameter. Obviously, the truncated system of (1.19) is equivalent to either (1.14) (in the cases in which $s = -1$) or (1.16) (in the cases in which $s = 1$). Thus, the bifurcation direction and stability of bifurcated periodic solutions are determined by the signs of $\mathrm{Re}\{\lambda'(0)\}$ and $\mathrm{Re}\{C(0)\}$ (or equivalently, $l_1(0)$).

1.5 Transcritical and Pitchfork Bifurcations of Equilibria

In a saddle-node bifurcation, on one side of a parameter value there is no equilibrium, and on the other side there are two equilibria. In some examples, we may meet another type of bifurcation: both equilibria exist before and after the bifurcation value, and there is one unstable equilibrium and one stable one; however, their stability is exchanged when they collide. So the unstable equilibrium becomes stable and vice versa. We refer to this type as a *transcritical bifurcation*, as shown in the following example.

Example 1.5. Consider a vector field

$$\dot{x} = \mu x - x^2, \quad x, \mu \in \mathbb{R}.$$

If $\mu < 0$, there are two equilibria: $x = 0$, which is stable, and $x = \mu$, which is unstable. These two equilibria coalesce at the bifurcation value $\mu = 0$. If $\mu > 0$, there are also two equilibria: $x = 0$ is unstable, while $x = \mu$ is stable. The bifurcation diagram is depicted in Fig. 1.3.

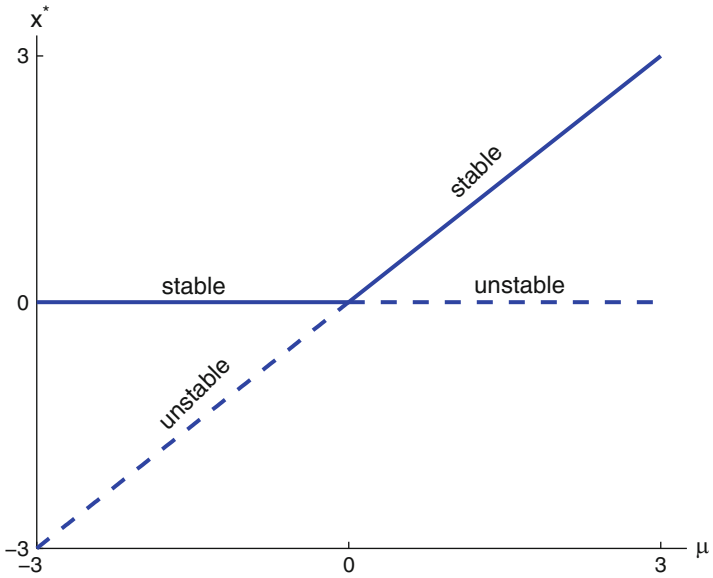

Fig. 1.3 Bifurcation diagram of a transcritical bifurcation

Similarly to the proof of Theorem 1.5, we may list sufficient conditions for a transcritical bifurcation for the scalar system (1.9).

Theorem 1.7. *Suppose f in (1.9) is sufficiently smooth and satisfies*

$$f(\mu, 0) = 0, \quad f_x(0,0) = 0, \quad f_{x\mu}(0,0) f_{xx}(0,0) \neq 0. \tag{1.20}$$

Then there are smooth invertible local coordinate and parameter changes that transform the system (1.9) into the following normal form:

$$\dot{y} = \gamma y \pm y^2 + O(|y|^3). \tag{1.21}$$

Therefore, besides the trivial solution, system (1.9) has a nonzero equilibrium, which continuously depends on μ for all sufficiently small $|\mu|$ and is stable for all sufficiently small μ such that $\mu f_{x\mu}(0,0) > 0$.

To illustrate another generic equilibrium bifurcation, we consider the following example.

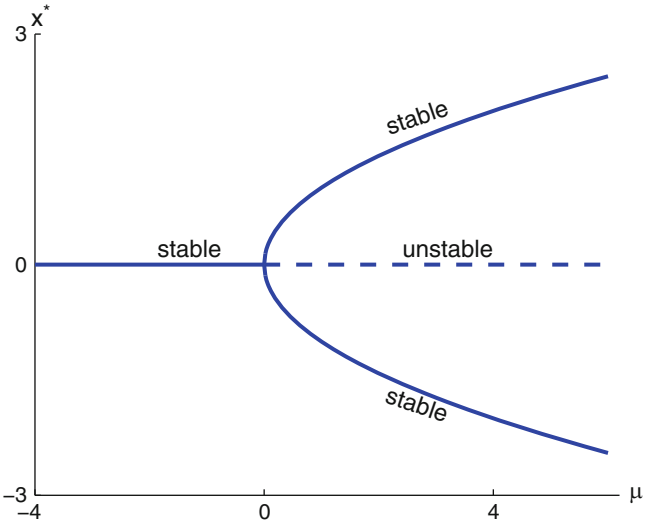

Fig. 1.4 Bifurcation diagram of a pitchfork bifurcation

Example 1.6. The vector field

$$\dot{x} = \mu x - x^3, \qquad x, \mu \in \mathbb{R}$$

has one stable equilibrium $x = 0$ if $\mu < 0$, and it has an unstable equilibrium $x = 0$ and two stable equilibria $x = \pm\sqrt{\mu}$ if $\mu > 0$. See Fig. 1.4.

The bifurcation diagram is shown in Fig. 1.4, and this kind of bifurcation is known as a *pitchfork bifurcation*. Note that $x = 0$ is always an equilibrium. However, as the parameter μ passes through the bifurcation value $\mu = 0$, the equilibrium at the origin loses its stability and two new stable equilibria are bifurcated from the origin. This is also an example of spontaneous symmetry breaking, because the two bifurcated equilibria do not have the symmetry $\mathbb{Z}_2$ possessed by the system. Moreover, this pitchfork bifurcation is called *supercritical* because new equilibria exist for a parameter μ that is greater than the bifurcation value $\mu = 0$. When additional equilibria exist for a parameter μ smaller than the bifurcation value $\mu = 0$, the bifurcation is called *subcritical*. An example of a subcritical pitchfork bifurcation can be seen in the equation $\dot{x} = \mu x + x^3$.

Similarly, we may list sufficient conditions for a pitchfork bifurcation in the scalar system (1.9). A more general theorem on pitchfork bifurcation will be formulated and proved in Sect. 7.2.

Theorem 1.8. *Suppose f in (1.9) is sufficiently smooth and satisfies*

$$f(\mu, -x) = -f(\mu, x), \quad f_x(0,0) = 0, \quad f_{x\mu}(0,0) f_{xxx}(0,0) \neq 0. \tag{1.22}$$

Then there are smooth invertible local coordinate and parameter changes that transform the system (1.9) into the following normal form:

$$\dot{y} = \gamma y \pm y^3 + o(|y|^3). \tag{1.23}$$

Therefore, if $f_{x\mu}(0,0) f_{xxx}(0,0) < 0$ *(respectively,* > 0*), then two nontrivial equilibria exist for* $\mu > 0$ *(respectively,* < 0*), and only the trivial equilibrium continues to exist for* $\mu < 0$ *(respectively,* > 0*). Moreover, the two nontrivial equilibria coalesce into zero as* μ *goes to* 0*.*

Remark 1.2. The codimension of a bifurcation is the number of parameters that must be varied for the bifurcation to occur. It coincides with the number of transversality conditions. This also corresponds to the codimension of the parameter set for which the bifurcation occurs within the full space of parameters. Saddle-node bifurcations and Hopf bifurcations are the only generic local bifurcations that are really of codimension one, while transcritical and pitchfork bifurcations both have a higher codimension. However, transcritical and pitchfork bifurcations are also often thought of as begin of codimension one, because the normal forms (1.21) and (1.23) can be written with only one parameter.

Remark 1.3. In Theorems 1.7 and 1.8, we study the transcritical and pitchfork bifurcations of equilibria in the one-parameter scalar system (1.9). Based on center manifold reduction (Chap. 3) and normal form theory (Chap. 4), we can discuss these bifurcations in high-dimensional systems, even in infinite-dimensional systems such as functional differential equations. See Sect. 7.2 for more details.

1.6 Bifurcations of Closed Orbits

When (1.1) has a periodic orbit Γ_0 when $\mu = \mu_0$, one may also be interested in the qualitative behaviors of solutions of (1.1) in a neighborhood of the periodic orbit Γ_0 for the parameter μ near μ_0.

The so-called Poincaré map is a technical tool for studying the local behaviors of solutions of (1.1) near a periodic orbit. To describe this tool, we consider a local transversal section L_ε to the periodic orbit Γ_0 (see Fig. 1.5). There are $\alpha_0 > 0$ and $\delta > 0$ such that for $0 \le |\mu - \mu_0| < \alpha_0$ and $x_0 \in L_\delta$, there is a first time $T(\mu, x_0) > 0$ such that the solution $x(t;\mu,x_0)$ of (1.1) satisfies $x(T(\mu,x_0);\mu,x_0) \in L_\varepsilon$. Therefore, we define the Poincaré map depending on parameters as $\Pi(\mu,x_0) = x(T(\mu,x_0);\mu,x_0)$ mapping L_δ to L_ε. Periodic orbits near Γ_0 correspond to fixed points of $\Pi(\mu,x_0)$. The periodic orbit through the point $x_0 \in L_\delta$ is said to be hyperbolic if x_0 is a hyperbolic fixed point of the Poincaré map $\Pi(\mu_0,\cdot)$, that is, none of the eigenvalues of the linearized operator $D_x\Pi(\mu_0,x_0)$ (also referred to as Floquet multipliers) lie on the unit circle.

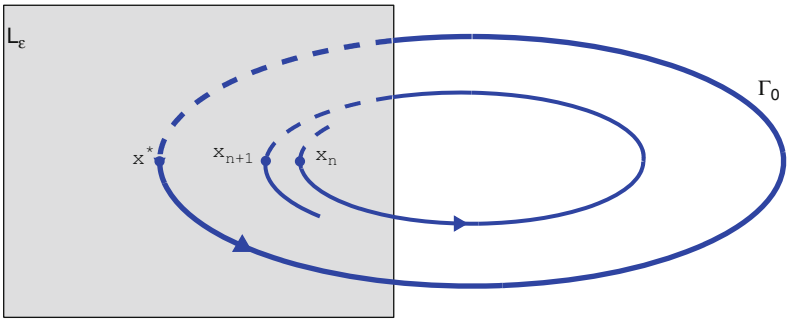

Fig. 1.5 An illustration of the Poincaré map for a periodic orbit, where x_{n+1} is the image of x_n under the Poincaré map

By means of the Poincaré map, we can investigate the behavior of solutions near a periodic solution. If Γ_0 is hyperbolic, then for each μ with $|\mu - \mu_0|$ small, there is a unique periodic orbit Γ_μ near Γ_0, and Γ_μ is also hyperbolic. When Γ_0 is nonhyperbolic, the bifurcations near the periodic orbit Γ_0 can be determined from those of the Poincaré map $\Pi(\mu, x_0)$.

Example 1.7 (Saddle-node bifurcation of periodic orbits). Consider the planar system

$$\begin{aligned} \dot{x} &= \mu x - y + x(x^2+y^2)(1-x^2-y^2), \\ \dot{y} &= x + \mu y + y(x^2+y^2)(1-x^2-y^2), \end{aligned} \tag{1.24}$$

where $x, y, \mu \in \mathbb{R}$. In polar coordinates $x + \mathrm{i}y = re^{\mathrm{i}\theta}$, the system (1.24) has the form

$$\begin{aligned} \dot{r} &= r(\mu + r^2 - r^4), \\ \dot{\theta} &= 1. \end{aligned} \tag{1.25}$$

Since the two equations above are uncoupled, we may investigate directly the local fold bifurcations for the r-equation using the general arguments in Sect. 1.4. However, the r-equation is so special that we can employ the following arguments to depict the global bifurcation explicitly and directly.

Indeed, if $\mu = -0.25$, then the periodic orbit is given by $r = \frac{\sqrt{2}}{2}$, and the transversal section L becomes

$$L = \{(r, \theta) \in \mathbb{R} \times \mathbb{S}^1 : r > 0, \theta = 0\}.$$

So the poincaré map $\Pi(-0.25, r)$ has a fixed point at $r = \frac{\sqrt{2}}{2}$. Moreover, it is easy to see that $D_r\Pi(-0.25, \frac{\sqrt{2}}{2}) = 1$. Consequently, the corresponding periodic orbit is nonhyperbolic. Moreover, since the first equation is independent of θ, it is easy to see that in the radial direction, system (1.25) undergoes a saddle-node bifurcation as the parameter μ passes through -0.25. If $\mu \in (-0.25, 0)$, system (1.25) has two periodic orbits: a stable periodic orbit $r = \sqrt{0.5 + \sqrt{\mu + 0.25}}$ and an unstable periodic orbit $r = \sqrt{0.5 - \sqrt{\mu + 0.25}}$. If $\mu < -0.25$, then system (1.25) has no periodic orbits, because $\dot{r} < 0$ and all the solutions tend to the origin as $t \to \infty$; see

Fig. 1.6. At the bifurcation value $\mu = -0.25$, there is only one semistable periodic orbit $r = \frac{\sqrt{2}}{2}$, which is not hyperbolic and has a Floquet multiplier equal to one.

For a nonhyperbolic periodic orbit of a higher-dimensional continuous dynamical system, there may be some bifurcations of closed orbits, which cannot happen in a planar system. For example, if at $\mu = \mu_0$, the closed orbit has a Floquet multiplier -1 and the modulus of all the remaining Floquet multipliers are not equal to 1, then a period-doubling bifurcation (also referred to as flip or subharmonic bifurcation) of the closed orbit may take place (see Fig. 1.7). Namely, as μ passes through μ_0, the closed orbit Γ_0 becomes another closed orbit Γ_μ with approximately twice the period of Γ_0. See Arnold [19], Newhouse–Palis–Takens [230], Feigenbaum [94] for further information. If at $\mu = \mu_0$ the closed orbit Γ_0 has a pair of complex conjugate Floquet multipliers on the unit circle, then as μ passes through μ_0, this nonhyperbolic closed orbit may bifurcate into a two-dimensional invariant torus Γ_μ (or $\mathbb{T}^2$). This bifurcation has many names. Some call it Neimark–Sacker bifurcation, while others call it the secondary Andronov–Hopf bifurcation due to its similarity to that for flows discussed in the previous section. Detailed analysis of Neimark–Sacker bifurcations can be found in Ruelle and Takens [256], Sacker [258], and Kuznetsov [200]. For details and further results on periodic orbits and their bifurcations, see, for example, [17, 63, 64, 98–102, 121, 122, 143, 151–155, 185, 212–214, 225, 288].

1.7 Homoclinic Bifurcation

A homoclinic orbit of a system is given by the intersection of the stable and unstable manifolds of a saddle-type invariant set (see Andronov and Leontovich [15], Kuznetsov [200]). Recall that the stable manifold is defined as the set of all trajectories that tend to the invariant set in forward time, and the unstable manifold is defined as the set of all trajectories that tend to the invariant set in backward time. Here, the invariant sets that we consider are steady states (equilibria) and/or periodic solutions.

For example, an orbit Γ_0 starting at a point $x \in \mathbb{R}$ is called homoclinic to the equilibrium x_0 of system (1.1) with $\mu = \mu_0$ if the solution $\varphi(t;x,\mu_0)$ tends to x_0 as $t \to \pm\infty$. In particular, if at $\mu = \mu_0$, system (1.1) has a homoclinic loop Γ_0, and the intersection of the stable and unstable manifolds of equilibria or closed orbits of system is not transversal,[1] then system (1.1) is not structurally stable. A slight perturbation of the parameter μ makes the stable and unstable manifolds either nonintersecting or transversally intersecting, and so may change the topological structure of the vector field of (1.1). Thus, closed orbits can be created or destroyed, and time-dependent behaviors such as invariant tori and even chaotic dynamics can be created. Therefore, a homoclinic orbit to a steady state is of codimension one; it may be destroyed by small perturbations to the system parameters.

[1] Two smooth manifolds $M, N \in \mathbb{R}^n$ intersect transversally if there exist n linearly independent vectors that are tangent to at least one of these manifolds at every intersection point.

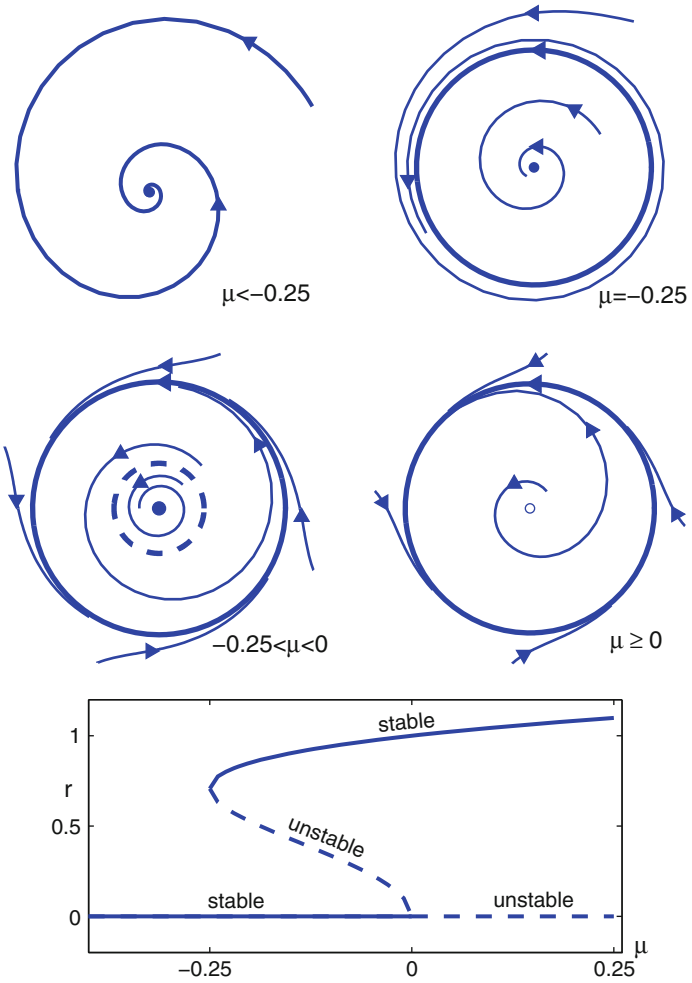

Fig. 1.6 The bifurcation phenomena of system (1.24)

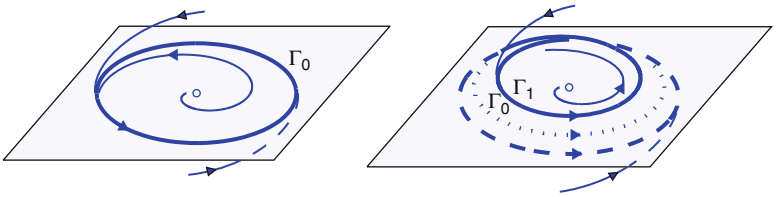

Fig. 1.7 Period-doubling bifurcation of a closed orbit

However, if a homoclinic orbit to a periodic solution is the transversal intersection of the stable and unstable manifolds of the periodic solution (Kuznetsov [200, Sects. 6.1 and 7.2.1]), then it cannot be destroyed by a small perturbation, but it can be destroyed through a codimension-one homoclinic tangency. This occurs when the intersection of the stable and unstable manifolds becomes tangential, and thus a small perturbation can separate the manifolds completely. A transition between a homoclinic orbit of a saddle-focus-type steady state and a homoclinic orbit of a periodic solution occurs at a codimension-two Shil'nikov–Hopf bifurcation (see Hirschberg and Knobloch [165]). At the Shil'nikov–Hopf bifurcation, the homoclinic orbit is *transferred* from the steady state to the periodic solution.

Example 1.8 (Periodic orbit from a homoclinic loop). Consider the planar system

$$\begin{aligned} \dot{x} &= 2y, \\ \dot{y} &= 2x - 3x^2 - y(x^3 - x^2 + y^2 - \mu), \end{aligned} \tag{1.26}$$

where $x, y, \mu \in \mathbb{R}$. For all values of μ, system (1.26) always has two equilibria: one saddle $(0,0)$ and one source $(2/3,0)$ when $\mu > -4/27$. When $\mu = 0$, we can employ Lyapunov functions $V(x,y) = x^3 - x^2 + y^2$ and phase portrait analysis to show that system (1.26) has a homoclinic orbit loop through the origin and attracts from inside, as seen in Fig. 1.8. For $-4/27 < \mu < 0$, using the invariance principle, one can show that there is an orbitally asymptotically stable periodic orbit lying on the curves $x^3 - x^2 + y^2 - \mu = 0$. As μ increases and tends to zero, the periodic orbit grows until it collides with the saddle point. At the bifurcation point $\mu = 0$, the period of the periodic orbit has grown to infinity, and it has become a homoclinic orbit. For $\mu > 0$, the homoclinic loop is broken, and also there is no periodic orbit. This sequence of bifurcations is illustrated in Fig. 1.8. Therefore, there is a homoclinic bifurcation at $\mu = 0$.

A homoclinic bifurcation often occurs when a periodic orbit collides with a saddle point. Homoclinic bifurcations can occur supercritically or subcritically. In three or more dimensions, bifurcations of higher codimension can occur, producing complicated, possibly chaotic, dynamics [297, 298].

1.8 Heteroclinic Bifurcation

An orbit Γ_0 starting at a point $x \in \mathbb{R}$ is called heteroclinic to the equilibria x_1 and $x_2 \neq x_1$ of system (1.1) with $\mu = \mu_0$ if the solution $\varphi(t; x, \mu_0)$ tends to x_1 as $t \to \infty$ and to x_2 as $t \to \infty$. The nontransversal heteroclinic case is somehow trivial, since the disappearance of the connecting orbit is the only essential event in a sufficiently small neighborhood of $\Gamma_0 \cup \{x_1, x_2\}$ (see Example 1.9).

Example 1.9 (Heteroclinic bifurcation). Consider the planar system

$$\begin{aligned} \dot{x} &= x^2 - y^2 - 1, \\ \dot{y} &= \mu + y^2 - xy, \end{aligned} \tag{1.27}$$

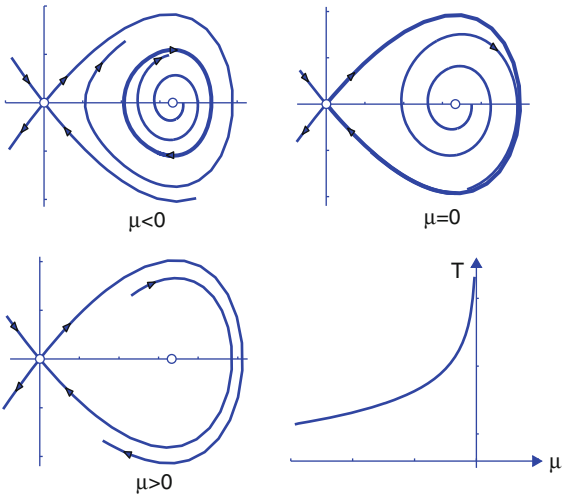

Fig. 1.8 Bifurcation phenomena in (1.26)

where $x, y, \mu \in \mathbb{R}$. When $\mu = 0$, system (1.27) has a heteroclinic trajectory connecting the two saddle points $(1,0)$ and $(-1,0)$. However, there is no heteroclinic trajectory when $\mu \neq 0$. Therefore, there is a heteroclinic bifurcation at $\mu = 0$ (Fig. 1.9).

1.9 Two-Parameter Bifurcations of Equilibria

Here we briefly review the generic bifurcations in two-parameter families of differential equations. We only give a list for them, and refer to Kuznetsov [200, 201], Guckenheimer [126], or Guckenheimer and Holmes [125] for analysis. There are two categories of generic bifurcations in two-parameter families: (1) extra eigenvalues can approach the imaginary axis; (2) some of the genericity con-

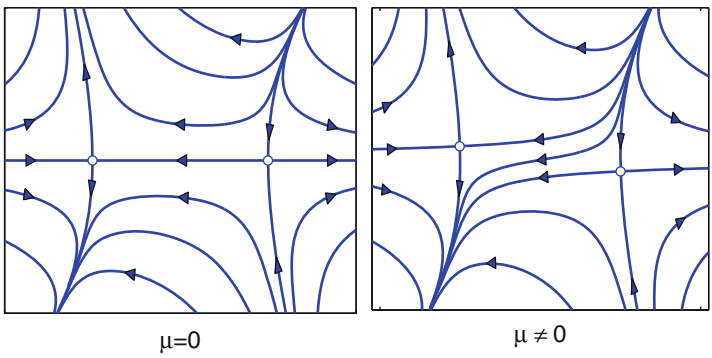

Fig. 1.9 Bifurcation phenomena in (1.27)

ditions for the codimension-one bifurcations can be violated. Thus, we can identify five bifurcation (Bogdanov–Takens bifurcation, cusp bifurcation, Bautin bifurcation, fold-Hopf bifurcation, and Hopf–Hopf bifurcation) points that one can meet in generic two-parameter systems while moving along codimension-one curves. Each of these bifurcations is characterized by two independent conditions. This section is devoted to the study of these bifurcations in the least possible phase-space dimensions.

1.9.1 Bogdanov–Takens Bifurcation

The Bogdanov–Takens bifurcation is a bifurcation of an equilibrium point in a two-parameter family of autonomous ODEs at which the critical equilibrium has a zero eigenvalue of (algebraic) multiplicity two. It is named after Rifkat Bogdanov and Floris Takens, who independently and simultaneously described this bifurcation. The main features of Bogdanov–Takens bifurcation were known to mathematicians of the Andronov school in the late 1960s. However, the complete picture is due to Bogdanov [35], as announced by Arnold [20] and Takens [274]. Their analysis is based on the Pontryagin [249] technique.

The usual normal form of the Bogdanov–Takens bifurcation is

$$\begin{aligned} \dot{x} &= y, \\ \dot{y} &= \mu_1 + \mu_2 x + x^2 \pm xy + O(\sqrt{(x^2+y^2)^3}), \end{aligned}$$

which was introduced by Bogdanov (see Sect. 7.4.2 for more details), while the normal form derived by Takens is

$$\begin{aligned} \dot{x} &= y + \mu_2 x + x^2 + O(\sqrt{(x^2+y^2)^3}), \\ \dot{y} &= \mu_1 \pm x^2 + O(\sqrt{(x^2+y^2)^3}). \end{aligned}$$

These two systems are equivalent, and their detailed analysis can be found, for example, in Guckenheimer and Holmes [125] and Kuznetsov [200]. In the above systems, four associated bifurcation curves meet at the Bogdanov–Takens bifurcation: two branches of the saddle-node bifurcation curve, an Andronov–Hopf bifurcation curve, and a saddle homoclinic bifurcation curve. Moreover, these bifurcations are nondegenerate, and no other bifurcations occur in a small fixed neighborhood of $(x,y) = (0,0)$ for parameter values sufficiently close to $\mu = 0$. In this neighborhood, the system has at most two equilibria and one limit cycle.

If system (1.1) has a fixed equilibrium $x = x_0$ for all parameters μ, and the equilibrium x_0 has a zero eigenvalue of (algebraic) multiplicity two at $\mu = 0$, then the normal form of (1.1) at $(\mu, x) = (0, x_0)$ is not equivalent to the above two systems derived by Bogdanov or Takens. See Sect. 7.4.3 for more details. Therefore, the goal of this subsection is to investigate the following two-parameter system:

$$\begin{aligned} \dot{x} &= y, \\ \dot{y} &= \mu_1 x + \mu_2 y + x^2 + xy, \end{aligned} \tag{1.28}$$

where $(\mu_1,\mu_2) \in \mathbb{R}^2$. At $(\mu_1,\mu_2) = (0,0)$, the linearization of (1.28) at the equilibrium $O = (0,0)$ has exactly one eigenvalue 0 of geometric multiplicity one and algebraic multiplicity two. The critical point $(\mu_1,\mu_2) = (0,0)$ is referred to as a Bogdanov–Takens point.

It is easy to see that system (1.28) always has two equilibria: $O = (0,0)$ and $E = (-\mu_1,0)$. Moreover, the characteristic equation of (1.28) at the equilibria O and E are $\lambda^2 - \mu_2\lambda - \mu_1 = 0$ and $\lambda^2 - (\mu_2 - \mu_1)\lambda + \mu_1 = 0$, respectively. Each of these two equations can have between zero and two real roots. However, the discriminant parabolas $\{(\mu_1,\mu_2) : \mu_2^2 + 4\mu_1 = 0\}$ and $\{(\mu_1,\mu_2) : (\mu_2 - \mu_1)^2 - 4\mu_1 = 0\}$ are not bifurcation curves at which the equilibrium O or E undergoes a node to focus transition. Moreover, it is easy to see that the equilibrium O (respectively, E) is a saddle for all parameters $\mu_1 > 0$ (respectively, $\mu_1 < 0$).

We can check that the equilibria O and E have a pair of purely imaginary eigenvalues on the lines $l_1 = \{(\mu_1,\mu_2) : \mu_1 < 0, \mu_2 = 0\}$ and $l_2 = \{(\mu_1,\mu_2) : \mu_1 = \mu_2 \geq 0\}$, respectively. This implies that the equilibrium O (or E) undergoes a nondegenerate Hopf bifurcation along the line l_1 (respectively, l_2), giving rise to an unstable limit cycle, since the first Lyapunov coefficients are both $1/|\mu_1| > 0$. The cycle exists near l_1 (or l_2) for $\mu_2 < 0$ (respectively, $\mu_2 < \mu_1$). We have the following results on the existence of a homoclinic bifurcation.

Theorem 1.9. *There exist exactly two smooth curves m_1 and m_2 corresponding to saddle homoclinic bifurcations in system (1.28) that originate at $(\mu_1,\mu_2) = (0,0)$ and have the following local representation:*

$$m_1 = \left\{(\mu_1,\mu_2) : \mu_2 = \frac{1}{7}\mu_1 + o(|\mu_1|),\ \mu_1 \leq 0\right\}$$

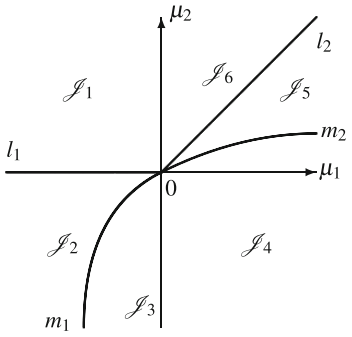

Fig. 1.10 Bifurcation sets for (1.28)

and

$$m_2 = \left\{(\mu_1,\mu_2) : \mu_2 = \frac{6}{7}\mu_1 + o(|\mu_1|),\ \mu_1 \geq 0\right\}.$$

Moreover, for $\|(\mu_1,\mu_2)\|$ small, system (1.28) has a unique and hyperbolic unstable cycle for parameter values inside the region bounded by the Hopf bifurcation curve

l_1 (or l_2) and the homoclinic bifurcation curve m_1 (respectively, m_2), and no cycles outside these regions.

Proof. First, we restrict our attention to the parameter region $\mathscr{J}_2$ in Fig. 1.10. Performing a singular rescaling and introducing a new time

$$u = x/(-\mu_1), \quad v = y/\sqrt{(-\mu_1)^3}, \quad s = t\sqrt{(-\mu_1)},$$

reduces (1.28) to

$$\begin{aligned} \dot{u} &= v, \\ \dot{v} &= u(u-1) - (\gamma_1 v + \gamma_2 uv), \end{aligned} \tag{1.29}$$

where the dots mean derivatives with respect to the new time s and

$$\gamma_1 = -\mu_2/\sqrt{(-\mu_1)}, \quad \gamma_2 = -\sqrt{(-\mu_1)}. \tag{1.30}$$

Clearly, system (1.29) is orbitally equivalent to a system induced by (1.28) with the help of (1.30). Studying the limit cycles and homoclinic orbits of (1.29) for $(\gamma_1, \gamma_2) \neq (0,0)$ provides complete information on these objects in (1.28). As stated in Kuznetsov 1998 [200, Sect. 8.8], there is a unique smooth curve m corresponding to a saddle homoclinic bifurcation in system (1.29) that originates at $(\gamma_1, \gamma_2) = (0,0)$ and has the following local representation:

$$m = \left\{ (\gamma_1, \gamma_2) : \gamma_1 = -\frac{1}{7}\gamma_2 + o(|\gamma_2|), \gamma_2 \leq 0 \right\}.$$

This homoclinic curve is mapped by (1.30) into the curve m_1. Using arguments similar to those in Kuznetsov 1998 [200, Sect. 8.8], we see that the cycle in (1.28) is unique and hyperbolic within the region bounded by l_1 and m_1.

In what follows, we focus on the parameter region $\mathscr{J}_5$, where O is a saddle and E is a stable focus. Translate the origin of the coordinate system to the left (antisaddle) equilibrium E of system (1.28):

$$\xi_1 = x + \mu_1, \quad \xi_2 = y.$$

This obviously gives

$$\begin{aligned} \dot{\xi}_1 &= \xi_2, \\ \dot{\xi}_2 &= -\mu_1\xi_1 + (\mu_2 - \mu_1)\xi_2 + \xi_1^2 + \xi_1\xi_2. \end{aligned} \tag{1.31}$$

Performing a singular rescaling and introducing a new time

$$u = x/\mu_1, \quad v = y/\sqrt{\mu_1^3}, \quad s = t\sqrt{\mu_1}$$

reduces (1.31)–(1.29) with

$$\gamma_1 = (\mu_1 - \mu_2)/\sqrt{\mu_1}, \quad \gamma_2 = -\sqrt{\mu_1}. \tag{1.32}$$

Thus, the homoclinic curve m is mapped by (1.32) into the curve m_2. Similarly, the cycle in (1.28) is unique and hyperbolic within the region bounded by l_2 and m_2. □

Thus, for $(\mu_1,\mu_2) \in m_2$ (or $(\mu_1,\mu_2) \in m_1$), there is an orbit homoclinic to the equilibrium O (respectively, E). In fact, we can also have nearly explicit expressions for the homoclinic orbits. Scaling system (1.28) by

$$t^* = \varepsilon t, \quad x^* = x/\varepsilon^2, \qquad \mu_1^* = \mu_1/\varepsilon^2, \quad \mu_2^* = \mu_2/\varepsilon^2,$$

and then dropping the $*$ gives

$$x'' - \varepsilon[\mu_2 x' + x x'] - (\mu_1 x + x^2) = O(\varepsilon^2). \tag{1.33}$$

Letting $\varepsilon = 0$, the equation has an explicit homoclinic orbit for $\mu_1 > 0$:

$$x = -\frac{2\mu_1}{2}\left[1 - \tanh^2\left(\frac{\sqrt{\mu_1}}{2}t\right)\right].$$

Using the Melnikov method (see, for example, Guckenheimer and Holmes 1983 [125]), we can compute parameter values for which the homoclinic orbit to the equilibrium O persists for ε. Moreover, the nearly explicit expressions for the homoclinic orbit to the equilibrium E can be discussed analogously.

Make a round trip near the Bogdanov–Takens point $(\mu_1,\mu_2) = (0,0)$ (see Fig. 1.10), starting from region $\mathscr{J}_1$, where equilibrium E is a saddle. There is a nonbifurcation curve (not shown in the figure) located in $\mathscr{J}_1$ and passing through the origin at which the equilibrium O undergoes an unstable node to an unstable focus transition. Entering from region $\mathscr{J}_1$ into region $\mathscr{J}_2$ through the Hopf bifurcation boundary l_1, the unstable focus O gains stability, and an unstable limit cycle $\mathscr{O}_1$ is present for sufficiently small parameters $|\mu_1|$ and $|\mu_2|$ satisfying $\mu_1 < 0$ and $\mu_2 < 0$. If we continue the journey counterclockwise, the unstable limit cycle $\mathscr{O}_1$ grows and approaches the saddle, turning into a homoclinic orbit at m_1. There are no cycles in region $\mathscr{J}_3$, where the equilibrium E remains a saddle while the stable focus O becomes a stable node. Entering from region $\mathscr{J}_3$ into region $\mathscr{J}_4$ through the negative μ_2-axis, the two equilibria O and E coalesce into zero and then exchange their properties, i.e., the stable node O becomes a saddle, while the saddle E becomes a stable node. In region $\mathscr{J}_4$, the equilibrium O remains a saddle, while the stable node E becomes a stable focus. Due to Theorem 1.9, system (1.28) has a homoclinic orbit at the curve m_2. As (μ_1,μ_2) continues moving counterclockwise in region $\mathscr{J}_5$, the homoclinic orbit turns into an unstable limit cycle, which shrinks and collides with equilibrium E and then disappears at the curve l_2. In region $\mathscr{J}_6$, the unstable focus E turns into an unstable node, while O remains a saddle.

1.9.2 Cusp Bifurcation

Cusp bifurcation is a bifurcation of equilibria in a two-parameter family of autonomous ODEs at which the critical equilibrium has one zero eigenvalue and the quadratic coefficient for the saddle-node bifurcation vanishes. Let us begin by considering the following example.

Example 1.10. Consider the following two-parameter system

$$\dot{x} = \mu_1 + \mu_2 x - x^3, \quad (x, \mu_1, \mu_2) \in \mathbb{R}^3. \tag{1.34}$$

At $(\mu_1, \mu_2) = (0,0)$, the linearization of (1.34) at the equilibrium 0 has exactly a simple eigenvalue 0. The critical point $(\mu_1, \mu_2) = (0,0)$ is referred to as a cusp point. The local bifurcation diagram of (1.34) is presented in Fig. 1.11. The cusp point $(\mu_1, \mu_2) = (0,0)$ is the origin of two branches of the saddle-node bifurcation curve:

$$LP_{\pm} = \{(\mu_1, \mu_2) : \mu_1 = \mp \frac{2}{3\sqrt{3}} \mu_2^{3/2}, \mu_2 > 0\},$$

which divides the parameter plane into two regions $\mathscr{J}_{1,2}$. Inside the region $\mathscr{J}_1$, there are three equilibria, two stable and one unstable. In the region $\mathscr{J}_2$, there is a single equilibrium, which is stable. A nondegenerate fold bifurcation (with respect to the parameter μ_1) takes place if we cross either LP_+ or LP_- at any point other than the origin. More precisely, if the curve LP_+ is crossed from region $\mathscr{J}_1$ to region $\mathscr{J}_2$, the right stable equilibrium collides with the unstable one, and then both disappear. The same happens to the left stable equilibrium and the unstable equilibrium at the curve LP_-. In the symmetric case $\mu_1 = 0$, one observes a pitchfork bifurcation as μ_2 is reduced, with one stable solution suddenly splitting into two stable solutions and one unstable solution as the physical system passes to $\mu_2 > 0$ through the cusp point $\mu = 0$ (an example of *spontaneous symmetry breaking*). In other words, if we approach the cusp point from inside the region $\mathscr{J}_1$, all three equilibria merge together into a triple root of the right-hand side of (1.34). Away from the cusp point, there is no sudden change in a physical solution being followed: when passing through the curve of saddle-node bifurcations, all that happens is that an alternative second solution becomes available.

In view of the above example, at the cusp bifurcation point, two branches of the saddle-node bifurcation curve meet tangentially, forming a semicubic parabola. For nearby parameter values, the system can have three equilibria that collide and disappear pairwise via the saddle-node bifurcations. The cusp bifurcation implies the presence of a hysteresis phenomenon.

Cusp bifurcation occurs also in infinite-dimensional ODEs generated by PDEs and DDEs, to which the center manifold theorem (see Chap. 3) applies. See Arrowsmith and Place [21] for details. The nomenclature and analysis of cusp bifurcations is based on cusps in singularity theory, where they appear as one of Thom's seven elementary catastrophes [275, 276]. The following theorem lists sufficient conditions for a general one-dimensional ODE.

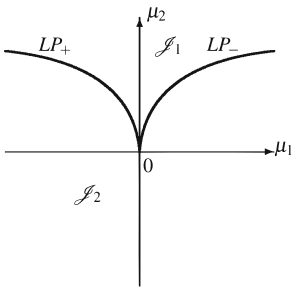

Fig. 1.11 Bifurcation sets for (1.34)

Theorem 1.10. *Suppose the system*

$$\dot{x} = f(\mu, x), \quad x \in \mathbb{R},\ \mu = (\mu_1, \mu_2) \in \mathbb{R}^2, \tag{1.35}$$

with a smooth function f, has at $\mu = 0$ the equilibrium $x = 0$ for which the cusp bifurcation conditions are satisfied, namely, $f_x(0,0) = f_{xx}(0,0) = 0$. Assume that the following genericity conditions are satisfied:

$$f_{xxx}(0,0) \neq 0, \quad \det \begin{bmatrix} f_{\mu_1} & f_{\mu_2} \\ f_{x\mu_1} & f_{x\mu_2} \end{bmatrix}_{(\mu,x)=(0,0)} \neq 0. \tag{1.36}$$

Then there are smooth invertible coordinate and parameter changes transforming the system into

$$\dot{y} = \beta_1 + \beta_2 y + s y^3 + O(y^4), \tag{1.37}$$

where the $s = \mathrm{sign} f_{xxx}(0,0)$ and $O(y^4)$ terms depend smoothly on (β_1, β_2).

Proof. Expand f with respect to x around $\mu = 0$:

$$f(\mu, x) = f_0(\mu) + f_1(\mu)x + f_2(\mu)x^2 + f_3(\mu)x^3 + O(x^3),$$

where

$$f_j(\mu) = \frac{1}{j!}\frac{\partial^j f}{\partial x^j}(\mu, 0), \quad j = 0, 1, 2, \ldots.$$

Obviously, $f_0(0) = f(0,0) = 0$, $f_1(0) = f_x(0,0) = 0$, and $f_2(0) = \frac{1}{2} f_{xx}(0,0) = 0$. Set $\xi = x + \delta(\mu)$, where δ is a constant independent of t. Then (1.35) can be transformed into

$$\begin{aligned} \dot{\xi} = {} & [f_0(\mu) - f_1(\mu)\delta + \delta^2 \varphi(\mu, \delta)] + [f_1(\mu) - 2f_2(\mu)\delta + \delta^2 \phi(\mu, \delta)]\xi \\ & + [f_2(\mu) - 3f_3(\mu)\delta + \delta^2 \psi(\mu, \delta)]\xi^2 + [f_3(\mu) + \delta\theta(\mu, \delta)]\xi^3 + O(\xi^4) \end{aligned} \tag{1.38}$$

for some smooth functions φ, ϕ, ψ, and θ. Since $f_2(0) = 0$, we cannot use the implicit function theorem to select a function $\delta(\mu)$ to eliminate the linear terms in ξ in the above equation. However, in view of $f_3(0) = \frac{1}{6} f_{xxx}(0,0) \neq 0$, there is a smooth shift function $\delta(\mu)$, $\delta(0) = 0$, that annihilates the quadratic terms in the equation for all sufficiently small $\|\mu\|$. Indeed, let $F(\mu,\delta) = f_2(\mu) - 3f_3(\mu)\delta + \delta^2\psi(\mu,\delta)$. Then we have $F(0,0) = 0$ and $F_\delta(0,0) = -3f_3(0) \neq 0$. Therefore, the implicit function theorem gives the (local) existence and uniqueness of a smooth scalar function $\delta = \delta(\mu)$ such that $\delta(0) = 0$ and $F(\mu,\delta(\mu)) = 0$ for $\|\mu\|$ small enough. Now with $\delta(\mu)$ as constructed above, (1.38) contains no quadratic terms. Let $\gamma(\mu) = (\gamma_1(\mu), \gamma_2(\mu))$ be defined as

$$\begin{aligned}\gamma_1(\mu) &= f_0(\mu) - f_1(\mu)\delta(\mu) + \delta^2(\mu)\varphi(\mu,\delta(\mu)),\\ \gamma_2(\mu) &= f_1(\mu) - 2f_2(\mu)\delta(\mu) + \delta^2(\mu)\phi(\mu,\delta(\mu)).\end{aligned}$$

Clearly, $\gamma(0) = 0$, and the Jacobian matrix of the map $\gamma = \gamma(\mu)$ is nonsingular at $\mu = 0$:

$$\det\left(\frac{\partial\gamma}{\partial\mu}\right)\Big|_{\mu=0} = \det\begin{bmatrix} f_{\mu_1} & f_{\mu_2} \\ f_{x\mu_1} & f_{x\mu_2}\end{bmatrix}_{\mu=0} \neq 0. \tag{1.39}$$

Thus, the inverse function theorem implies the local existence and uniqueness of a smooth inverse function $\mu = \mu(\gamma)$ with $\mu(0) = 0$. Therefore, the equation for ξ now reads

$$\dot{\xi} = \gamma_1 + \gamma_2\xi + c(\gamma)\xi^3 + O(\xi^4),$$

where $c(\gamma) = f_3(\mu(\gamma)) + \delta(\mu((\gamma))\theta(\mu(\gamma),\delta(\mu(\gamma)))$ is a smooth function of γ and $c(0) = f_3(0) = \frac{1}{6} f_{xxx}(0,0) \neq 0$. Finally, the above equation can be transformed into (1.37) by performing a linear scaling $y = \xi\sqrt{|c(\gamma)|}$ and introducing new parameters: $\beta_1 = \gamma_1\sqrt{|c(\gamma)|}$, $\beta_2 = \gamma_2$. □

1.9.3 Fold–Hopf Bifurcation

The fold–Hopf bifurcation is a bifurcation of an equilibrium point in a two-parameter family of autonomous ODEs at which the critical equilibrium has a zero eigenvalue and a pair of purely imaginary eigenvalues. This phenomenon is also called the zero–Hopf bifurcation or Gavrilov–Guckenheimer bifurcation. An early example of this bifurcation in a specific system is provided by the Brusselator reaction–diffusion system in one spatial dimension (Guckenheimer [124], Wittenberg and Holmes [299]).

The usual norm form of the fold–Hopf bifurcation is

$$\begin{aligned} \dot{y} &= \mu_1 + b(u^2+v^2) - y^2 + \text{h.o.t.}, \\ \dot{u} &= \mu_2 u - v + ayu + \text{h.o.t.}, \\ \dot{v} &= u + \mu_2 v + ayv + \text{h.o.t.}, \end{aligned} \tag{1.40}$$

where $\mu = (\mu_1, \mu_2)$ and h.o.t. stands for "higher-order terms." System (1.40) has been studied by Broer and Vegter [44], Chow–Li–Wang [66], Dumortier and Ibáñez [84], Gamero–Freire–Rodríguez–Luis [106], Gaspard [107], Gavrilov [108, 109], Guckenheimer [124], Keener [187], Langford [202], Takens [272–274]. The bifurcation point $\mu = 0$ in the μ-parameter plane lies at a tangential intersection of curves of saddle-node bifurcations and Poincaré–Andronov–Hopf bifurcations. Depending on the system, a branch of torus bifurcations can emanate from the fold–Hopf bifurcation point. In such cases, other bifurcations occur for nearby parameter values, including saddle-node bifurcations of periodic orbits on the invariant torus, torus breakdown, and bifurcations of Shil'nikov homoclinic orbits to saddle-foci and heteroclinic orbits connecting equilibria. See Guckenheimer and Holmes [125] for more details.

If system (1.1) has a fixed equilibrium $x = x_0$ for all parameters μ, and the equilibrium x_0 has a zero eigenvalue and a pair of purely imaginary eigenvalues at $\mu = 0$, then the normal form of (1.1) at $(\mu, x) = (0, x_0)$ is not equivalent to system (1.40). Therefore, in this subsection we consider the following two-parameter system:

$$\begin{aligned} \dot{y} &= \mu_1 y + y^2 + u^2 + v^2, \\ \dot{u} &= \mu_2 u - v + ayu + y^2 u, \\ \dot{v} &= u + \mu_2 v + ayv + y^2 v, \end{aligned} \tag{1.41}$$

where $0 \neq a \in \mathbb{R}$, $\mu = (\mu_1, \mu_2) \in \mathbb{R}^2$, and $(y, u, v) \in \mathbb{R}^3$. At $\mu = 0$, the linearization of (1.41) at the equilibrium $(0,0,0)$ has a zero eigenvalue $\lambda_1 = 0$ and a pair of purely imaginary eigenvalues $\lambda_{2,3} = \pm \mathrm{i}$. Let $z = u + \mathrm{i}v = \sqrt{\rho}\mathrm{e}^{\mathrm{i}\theta}$. Then system (1.41) can be rewritten as

$$\begin{aligned} \dot{y} &= \mu_1 y + y^2 + |z|^2, \\ \dot{z} &= (\mu_2 + \mathrm{i})z + ayz + y^2 z, \end{aligned} \tag{1.42}$$

and

$$\begin{aligned} \dot{y} &= \mu_1 y + y^2 + \rho, \\ \dot{\rho} &= 2\rho(\mu_2 + ay + y^2), \\ \dot{\theta} &= 1. \end{aligned} \tag{1.43}$$

The first two equations of (1.43) are decoupled from the third one. The equation for θ describes a rotation around the y-axis with constant angular velocity $\dot{\theta} = 1$. Thus, to understand the bifurcations in (1.43), we only need to study the planar system for (y, ρ) with $\rho \geq 0$:

$$\begin{aligned} \dot{y} &= \mu_1 y + y^2 + \rho, \\ \dot{\rho} &= 2\rho(\mu_2 + ay + y^2). \end{aligned} \tag{1.44}$$

It is easy to see that system (1.44) always has two equilibria, $E_1 = (0,0)$ and $E_2 = (-\mu_1, 0)$, and that there always exists one orbit connecting E_1 and E_2 due to the symmetry that the y-axis is always invariant. Other equilibria (y,ρ) of (1.44) with $\rho > 0$ satisfy

$$\mu_1 y + y^2 + \rho = 0 \quad \text{and} \quad \mu_2 + ay + y^2 = 0, \tag{1.45}$$

which can have zero, one, or two solutions in the interior of the quadrants with $\rho > 0$. Since we consider the dynamics of (1.44) only with μ sufficiently close to 0, we can require the parameters μ to be in $\mathscr{J} = \{\mu = (\mu_1, \mu_2)\colon |\mu_1| < \frac{1}{2}|a|$ and $|\mu_2| < \frac{1}{4}a^2\}$. Thus, the second equation of (1.45) has two solutions y_1 and y_2 with $y_1 < y_2$. Moreover, $y_1 < y_2 < 0$ if $\mu_2 > 0$ and $a > 0$, while $y_1 < 0 < y_2$ if $\mu_2 < 0$ and $a > 0$. Next, we determine the signs of $\rho_j = -y_j^2 - \mu_1 y_j$, $j = 1,2$, because we consider the equilibrium (y,ρ) of (1.44) only with $\rho \geq 0$.

We first consider the case $a > 0$. We divide the region $\mathscr{J}$ into six parts:

$$\begin{aligned} \mathscr{J}_{11} &= \{\mu \in \mathscr{J} : \mu_1 < 0 \text{ and } \mu_2 > 0\}, \\ \mathscr{J}_{12} &= \{\mu \in \mathscr{J} : \mu_1 < 0 \text{ and } \mu_2 < 0 \text{ and } \mu_1^2 - a\mu_1 + \mu_2 > 0\}, \\ \mathscr{J}_{13} &= \{\mu \in \mathscr{J} : \mu_1 < 0 \text{ and } \mu_1^2 - a\mu_1 + \mu_2 < 0\}, \\ \mathscr{J}_{14} &= \{\mu \in \mathscr{J} : \mu_1 > 0 \text{ and } \mu_1^2 - a\mu_1 + \mu_2 > 0\}, \\ \mathscr{J}_{15} &= \{\mu \in \mathscr{J} : \mu_1 > 0 \text{ and } \mu_2 > 0 \text{ and } \mu_1^2 - a\mu_1 + \mu_2 < 0\}, \\ \mathscr{J}_{16} &= \{\mu \in \mathscr{J} : \mu_1 > 0 \text{ and } \mu_2 < 0\}. \end{aligned}$$

These regions are illustrated in Fig. 1.12a, where the bold curve l_4 represents the parabola $\mu_1^2 - \mu_1 a + \mu_2 = 0$.

Lemma 1.1. *Suppose $a > 0$. Then in the interior of the quadrants of the (y,ρ)-plane with $\rho > 0$, system (1.45) has no solution (respectively, one solution (y_2,ρ_2) with $y_2 > 0$, one solution (y_2,ρ_2) with $y_2 < 0$) for parameters μ in $\mathscr{J} \setminus (\mathscr{J}_{12} \cup \mathscr{J}_{15})$ (respectively, $\mathscr{J}_{12}$, $\mathscr{J}_{15}$).*

Proof. We distinguish two cases:

Case 1: $\mu_1 < 0$. Then $y^2 + \mu_1 y$ is negative if $0 < y < -\mu_1$ and positive otherwise. If $\mu \in \mathscr{J}_{11}$, then $y_1 < y_2 < 0$, and hence $\rho_j = -y_j^2 - \mu_1 y_1 < 0$, $j = 1,2$. If $\mu \in \mathscr{J}_{12}$, then $y_1 < 0 < y_2 < -\mu_1$, and hence $\rho_1 < 0$ and $\rho_2 > 0$. If $\mu \in \mathscr{J}_{13}$, then $y_1 < 0 < -\mu_1 < y_2$, and hence $\rho_j = -y_j^2 - \mu_1 y_1 < 0$, $j = 1,2$.

Case 2: $\mu_1 > 0$. Then $y^2 + \mu_1 y$ is negative if $-\mu_1 < y < 0$ and positive otherwise. If $\mu \in \mathscr{J}_{14}$, then $y_1 < y_2 < -\mu_1 < 0$, and hence $\rho_j < 0$, $j = 1,2$. If $\mu \in \mathscr{J}_{15}$, then $y_1 < -\mu_1 < y_2 < 0$, and hence $\rho_1 < 0$ and $\rho_2 > 0$. If $\mu \in \mathscr{J}_{16}$, then $y_1 < -\mu_1 < 0 < y_2$, and hence $\rho_1 < 0$ and $\rho_2 < 0$. The proof is complete. □

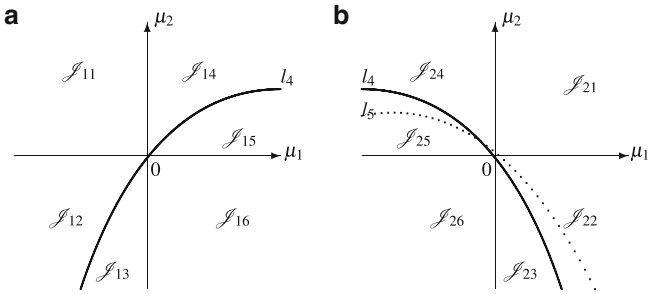

Fig. 1.12 Bifurcation sets for (1.44)

Moreover, for parameters $\mu \in \mathscr{J}_{12} \cup \mathscr{J}_{15}$, the characteristic equation of (1.44) at the equilibrium $E_3 = (y_2, \rho_2)$ is

$$\varsigma^2 - (\mu_1 + 2y_2)\varsigma - 2\rho_2(a + 2y_2) = 0.$$

The two eigenvalues $\varsigma_{1,2}$ satisfy $\varsigma_1\varsigma_2 = -2\rho_2(a + 2y_2)$. For $\mu \in \mathscr{J}_{12}$, it follows from the proof of Lemma 1.1 that $y_2 > 0$, and so $\varsigma_1\varsigma_2 < 0$. For $\mu \in \mathscr{J}_{15}$, it follows from the proof of Lemma 1.1 that $-\frac{1}{2}a < -\mu_1 < y_2 < 0$, and hence $\varsigma_1\varsigma_2 < 0$. Thus, we obtain the following:

Proposition 1.1. *Suppose $a > 0$. Then, in the quadrants of the (y, ρ)-plane with $\rho \geq 0$, we have the following information on the equilibria of system (1.44):*

(i) *There are two equilibria E_1 and E_2 for $\mu \in \mathscr{J}_{11}$, where E_1 is a saddle and E_2 is a source.*
(ii) *There are three equilibria E_1, E_2, and E_3 for $\mu \in \mathscr{J}_{12}$, where E_1 is a sink, E_2 is a source, $E_3 = (y_2, \rho_2)$ satisfying $y_2 > 0$ and $\rho_2 > 0$ is a saddle.*
(iii) *There are two equilibria E_1 and E_2 for $\mu \in \mathscr{J}_{13}$, where E_1 is a sink and E_2 is a saddle.*
(iv) *There are two equilibria E_1 and E_2 for $\mu \in \mathscr{J}_{14}$, where E_1 is a source and E_2 is a saddle.*
(v) *There are three equilibria E_1, E_2, and E_3 for $\mu \in \mathscr{J}_{15}$, where E_1 is a source, E_2 is a sink, $E_3 = (y_2, \rho_2)$ satisfying $y_2 < 0$ and $\rho_2 > 0$ is a saddle.*
(vi) *There are two equilibria E_1 and E_2 for $\mu \in \mathscr{J}_{16}$, where E_1 is a saddle and E_2 is a sink.*

The following theorem follows immediately from the equivalence mentioned before.

Theorem 1.11. *Suppose $a > 0$. Then a semistable limit cycle of (1.41) appears as μ crosses the negative μ_1-axis from $\mathscr{J}_{11}$ to $\mathscr{J}_{12}$, which is always present for $\mu \in \mathscr{J}_{12}$, and then disappears as μ crosses the parabola l_4 from $\mathscr{J}_{12}$ to $\mathscr{J}_{13}$. Similarly, a semistable limit cycle of (1.41) appears as μ crosses the parabola l_4 from $\mathscr{J}_{14}$ to $\mathscr{J}_{15}$, which is always present for $\mu \in \mathscr{J}_{15}$, and then disappears as μ crosses the positive μ_1-axis from $\mathscr{J}_{15}$ to $\mathscr{J}_{16}$.*

Now we consider the case $a<0$. Again, we divide the region $\mathscr{J}$ into six parts:

$$\begin{aligned}
\mathscr{J}_{21} &= \{\mu\in\mathscr{J}:\mu_1>0 \text{ and } \mu_2>0\},\\
\mathscr{J}_{22} &= \{\mu\in\mathscr{J}:\mu_1>0 \text{ and } \mu_2<0 \text{ and } \mu_1^2-\mu_1 a+\mu_2>0\},\\
\mathscr{J}_{23} &= \{\mu\in\mathscr{J}:\mu_1>0 \text{ and } \mu_1^2-\mu_1 a+\mu_2<0\},\\
\mathscr{J}_{24} &= \{\mu\in\mathscr{J}:\mu_1<0 \text{ and } \mu_1^2-\mu_1 a+\mu_2>0\},\\
\mathscr{J}_{25} &= \{\mu\in\mathscr{J}:\mu_1<0 \text{ and } \mu_2>0 \text{ and } \mu_1^2-\mu_1 a+\mu_2<0\},\\
\mathscr{J}_{26} &= \{\mu\in\mathscr{J}:\mu_1<0 \text{ and } \mu_2<0\}.
\end{aligned}$$

These regions are illustrated in Fig. 1.12b, where the bold curve l_4 and the dotted curve l_5 represent the parabolas $\mu_1^2-\mu_1 a+\mu_2=0$ and $\mu_1^2-2\mu_1 a+4\mu_2=0$, respectively. Similarly, we have the following result.

Lemma 1.2. *Suppose $a<0$. Then, in the interior of the quadrants of the (y,ρ)-plane with $\rho>0$, system (1.45) has no solution (respectively, one solution (y_1,ρ_1) with $y_1<0$, one solution (y_1,ρ_1) with $y_1>0$) for parameters μ in $\mathscr{J}\setminus(\mathscr{J}_{22}\cup\mathscr{J}_{25})$ (respectively, $\mathscr{J}_{22}$, $\mathscr{J}_{25}$).*

Moreover, for parameters $\mu\in\mathscr{J}_{22}\cup\mathscr{J}_{25}$, the characteristic polynomial of (1.44) at the equilibrium $E_4=(y_1,\rho_1)$ is

$$\varsigma^2-(\mu_1+2y_1)\varsigma-2\rho_1(a+2y_1)=0.$$

The two eigenvalues $\varsigma_{1,2}$ satisfy $\varsigma_1\varsigma_2=-2\rho_1(a+2y_1)$, which can be shown to be positive. Then, we need to consider the sign of $\varsigma_1+\varsigma_2$ in order to discuss the stability of the equilibrium E_4. In fact,

$$\varsigma_1+\varsigma_2=\mu_1+2y_1=\mu_1-a-\sqrt{a^2-4\mu_2}.$$

It follows from $2|\mu_1|<|a|$ and $a<0$ that $\mu_1-a>0$, and hence

$$\begin{aligned}
\operatorname{sign}(\varsigma_1+\varsigma_2) &= \operatorname{sign}\{(\mu_1-a)^2-a^2+4\mu_2\}\\
&= \operatorname{sign}\{\mu_1^2-2\mu_1 a+4\mu_2\}.
\end{aligned}$$

Let

$$\mathscr{J}^+=\{\mu:\mu_1^2-2\mu_1 a+4\mu_2>0\}$$

and

$$\mathscr{J}^-=\{\mu:\mu_1^2-2\mu_1 a+4\mu_2<0\}.$$

Then we have the following:

Lemma 1.3. *Suppose $a<0$. For parameters $\mu\in\mathscr{J}_{22}\cup\mathscr{J}_{25}$, besides equilibria E_1 and E_2, system (1.45) has a third equilibrium E_4, which is a sink if $\mu\in\mathscr{J}^-\cap(\mathscr{J}_{22}\cup\mathscr{J}_{25})$ and a source if $\mu\in\mathscr{J}^+\cap(\mathscr{J}_{22}\cup\mathscr{J}_{25})$.*

Proposition 1.2. *Suppose $a < 0$. Then, in the quadrants of the (y,ρ)-plane with $\rho \geq 0$, we have the following information about equilibria of system (1.44):*

(i) *There are two equilibria E_1 and E_2 for $\mu \in \mathscr{J}_{21}$, where E_1 is a source and E_2 is a saddle.*

(ii) *There are three equilibria E_1, E_2, and E_4 for $\mu \in \mathscr{J}_{22}$, where E_1 and E_2 are saddles, and $E_4 = (y_1, \rho_1)$ satisfying $y_1 < 0$ and $\rho_1 > 0$ is a sink if $\mu_1^2 - 2\mu_1 a + 4\mu_2 < 0$ and a source otherwise. Namely, in the region $\mathscr{J}_{22}$, as μ crosses the parabola l_5 from the region $\mathscr{J}_{22} \cap \mathscr{J}^+$ to the region $\mathscr{J}_{22} \cap \mathscr{J}^-$, the equilibrium E_4 gains stability, and hence system (1.44) undergoes a Hopf bifurcation, and a stable limit cycle appears; as μ varies further, this limit cycle can approach a heteroclinic cycle formed by the separatrices of the two saddles E_1 and E_2, i.e., its period tends to infinity and the cycle disappears.*

(iii) *There are two equilibria E_1 and E_2 for $\mu \in \mathscr{J}_{23}$, where E_1 is a saddle and E_2 is a sink.*

(iv) *There are two equilibria E_1 and E_2 for $\mu \in \mathscr{J}_{24}$, where E_1 is a saddle and E_2 is a source.*

(v) *There are three equilibria E_1, E_2, and E_4 for $\mu \in \mathscr{J}_{25}$, where E_1 and E_2 are saddles, and $E_4 = (y_1, \rho_1)$ satisfying $y_1 > 0$ and $\rho_1 > 0$ is a sink if $\mu_1^2 - 2\mu_1 a + 4\mu_2 < 0$ and a source otherwise. Namely, in the region $\mathscr{J}_{25}$, as μ crosses the parabola l_5 from the region $\mathscr{J}_{25} \cap \mathscr{J}^+$ to the region $\mathscr{J}_{25} \cap \mathscr{J}^-$, equilibrium E_4 gains stability, and hence system (1.44) undergoes a Hopf bifurcation, and a stable limit cycle appears; as μ varies further, this limit cycle can approach a heteroclinic cycle formed by the separatrices of the two saddles E_1 and E_2, i.e., its period tends to infinity, and the cycle disappears.*

(vi) *There are two equilibria E_1 and E_2 for $\mu \in \mathscr{J}_{26}$, where E_1 is a sink and E_2 is a saddle.*

Theorem 1.12. *Suppose that $a < 0$. Then the following statements are true:*

(i) *An unstable limit cycle $\mathscr{O}_1$ of (1.41) appears as μ crosses the positive μ_1-axis from $\mathscr{J}_{21}$ to $\mathscr{J}_{22}$. As μ crosses the parabola l_5 from $\mathscr{J}_{22} \cap \mathscr{J}^+$ to $\mathscr{J}_{22} \cap \mathscr{J}^-$, this limit cycle $\mathscr{O}_1$ becomes stable and generates an unstable torus $\mathscr{T}_1$. Under further variation of the parameter μ in $\mathscr{J}_{22} \cap \mathscr{J}^-$, this torus $\mathscr{T}_1$ degenerates to a sphere-like surface $\mathscr{S}_1$ and then disappears. As μ crosses the parabola l_4 from $\mathscr{J}_{22} \cap \mathscr{J}^-$ to $\mathscr{J}_{23}$, the stable limit circle $\mathscr{O}_1$ disappears.*

(ii) *An unstable limit cycle $\mathscr{O}_2$ of (1.41) appears as μ crosses the parabola l_4 from $\mathscr{J}_{24}$ to $\mathscr{J}_{25}$. As μ crosses the parabola l_5 from $\mathscr{J}_{25} \cap \mathscr{J}^+$ to $\mathscr{J}_{25} \cap \mathscr{J}^-$, this limit cycle $\mathscr{O}_2$ becomes stable and generates an unstable torus $\mathscr{T}_2$. Under further variation of the parameter μ in $\mathscr{J}_{25} \cap \mathscr{J}^-$, this torus $\mathscr{T}_2$ degenerates to a sphere-like surface $\mathscr{S}_2$ and then disappears. As μ crosses the negative μ_1-axis from $\mathscr{J}_{25} \cap \mathscr{J}^-$ to $\mathscr{J}_{26}$, the stable limit circle $\mathscr{O}_2$ disappears.*

1.9.4 Bautin Bifurcation

Consider the following two-parameter system:

$$\begin{aligned} \dot{x}_1 &= \mu_1 x_1 - x_2 + \mu_2 x_1 (x_1^2 + x_2^2) + \sigma x_1 (x_1^2 + x_2^2)^2, \\ \dot{x}_2 &= x_1 + \mu_1 x_2 + \mu_2 x_2 (x_1^2 + x_2^2) + \sigma x_2 (x_1^2 + x_2^2)^2, \end{aligned} \tag{1.46}$$

where $\sigma = \pm 1$, $\mu = (\mu_1, \mu_2) \in \mathbb{R}^2$, and $x = (x_1, x_2) \in \mathbb{R}^2$. At $\mu = 0$, the linearization of (1.46) at the equilibrium $(0,0)$ has a pair of purely imaginary eigenvalues $\pm \mathrm{i}$. Let $z = u + \mathrm{i}v = \sqrt{\rho} \mathrm{e}^{\mathrm{i}\theta}$. Then system (1.46) can be rewritten as

$$\dot{z} = (\mu_1 + \mathrm{i}) z + \mu_2 z |z|^2 + \sigma z |z|^4, \quad z \in \mathbb{C} \tag{1.47}$$

and

$$\begin{aligned} \dot{\rho} &= 2\rho(\mu_1 + \mu_2 \rho + \sigma \rho^2), \\ \dot{\theta} &= 1. \end{aligned} \tag{1.48}$$

The first equation in (1.48) is uncoupled from the second one. Thus, to understand the bifurcations in (1.48), it suffices to study the scalar equation for ρ, that is,

$$\dot{\rho} = 2\rho(\mu_1 + \mu_2 \rho + \sigma \rho^2). \tag{1.49}$$

It follows that the trivial equilibrium $\rho = 0$ of (1.49) corresponds to the equilibrium $x = 0$ of (1.46), and the existence and stability of positive equilibria of (1.49) determine the existence and stability of periodic solutions of (1.47) and hence of the original system (1.46). In the remaining part of this subsection, we depict the complete bifurcation diagrams of (1.49) on the μ-parameter plane.

We first consider the case $\sigma = -1$. Positive equilibria of (1.49) satisfy $\mu_1 + \mu_2 \rho - \rho^2 = 0$, which can have zero, one, or two positive solutions. These solutions branch from the trivial one along the line l_1 on the μ-parameter plane and collide and disappear at the half-parabola l_2 (see Fig. 1.13a),

where

$$l_1 : \mu_1 = 0 \quad \text{and} \quad l_2 : \mu_2^2 + 4\mu_1 = 0 \text{ with } \mu_2 > 0.$$

The details are summarized below.

1. In the region $\mathscr{D}_{11} = \{\mu : \mu_2^2 + 4\mu_1 < 0 \text{ or } \mu_1 < 0 \text{ and } \mu_2 < 0\}$, (1.49) has no positive equilibria. Thus, the equilibrium $\rho = 0$ is globally asymptotically stable, which means that system (1.46) has no periodic solutions in a sufficiently small neighborhood of the stable equilibrium $z = 0$.
2. In the region $\mathscr{D}_{12} = \{\mu : \mu_1 > 0\}$, (1.49) has only one positive equilibrium, which is stable. This means that system (1.46) has exactly one stable periodic solution in a sufficiently small neighborhood of the unstable equilibrium $x = 0$.
3. In the region $\mathscr{D}_{13} = \{\mu : \mu_1 < 0, \mu_2 > 0, \text{ and } \mu_2^2 + 4\mu_1 > 0\}$, (1.49) has two positive equilibria, one stable and the other unstable. This means that system (1.46) has one stable periodic solution and one unstable periodic solution in a sufficiently small neighborhood of the stable equilibrium $x = 0$.

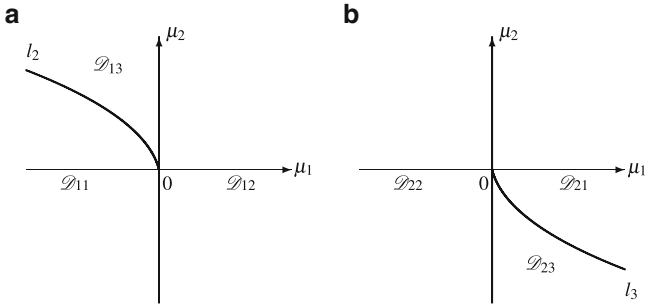

Fig. 1.13 Bifurcation sets for (1.49)

Therefore, on the μ-parameter plane, the line l_1 and the half-parabola l_2 are bifurcation curves. The bifurcation scenario is explained below.

(a) On the μ-parameter plane, if the point μ crosses the line l_1 from region $\mathscr{D}_{11}$ to region $\mathscr{D}_{12}$, then (1.46) undergoes a Hopf bifurcation, and a stable limit cycle bifurcates from $x = 0$.
(b) On the μ-parameter plane, if the point μ crosses the line l_1 from region $\mathscr{D}_{12}$ to region $\mathscr{D}_{13}$, then (1.46) undergoes a Hopf bifurcation, and an unstable limit cycle bifurcates from $x = 0$.
(c) On the μ-parameter plane, if the point μ crosses the line l_2 from region $\mathscr{D}_{13}$ to region $\mathscr{D}_{11}$, then limit cycles of (1.46) undergo a fold bifurcation, i.e., the two limit cycles collide and then disappear.

Now we come to the complete bifurcation diagram of (1.49) with $\sigma = 1$. Positive equilibria of (1.49) satisfy $\mu_1 + \mu_2\rho + \rho^2 = 0$, which can have zero, one, or two positive solutions. These solutions branch from the trivial one along the line l_1 on the μ-parameter plane and collide and disappear at the half-parabola $l_3 : \mu_2^2 - 4\mu_1 = 0$ and $\mu_2 < 0$ (see Fig. 1.13b). We have the following conclusions:

1. In the region $\mathscr{D}_{21} = \{\mu : \mu_2^2 - 4\mu_1 < 0 \text{ or } \mu_1 > 0 \text{ and } \mu_2 > 0\}$, (1.49) has no positive equilibria. Thus, the equilibrium $\rho = 0$ is unstable. This means that system (1.46) has no periodic solutions in a sufficiently small neighborhood of the unstable equilibrium $z = 0$.
2. In the region $\mathscr{D}_{22} = \{\mu : \mu_1 < 0\}$, (1.49) has only one positive equilibrium, which is unstable. This means that system (1.46) has exactly one unstable periodic solution in a sufficiently small neighborhood of the stable equilibrium $x = 0$.
3. In the region $\mathscr{D}_{23} = \{\mu : \mu_1 > 0, \mu_2 < 0, \text{ and } \mu_2^2 - 4\mu_1 > 0\}$, (1.49) has two positive equilibria, one stable and the other unstable. This means that system (1.46) has one stable periodic solution and one unstable periodic solution in a sufficiently small neighborhood of the unstable equilibrium $x = 0$.

Therefore, on the parameter plane μ, the line l_1 and the half-parabola l_3 are bifurcation curves. More specifically, we have the following:

(a) On the μ-parameter plane, if the point μ crosses the line l_1 from region $\mathscr{D}_{21}$ to region $\mathscr{D}_{22}$, then (1.46) undergoes a Hopf bifurcation, and an unstable limit cycle bifurcates from $x = 0$.
(b) On the μ-parameter plane, if the point μ crosses the line l_1 from region $\mathscr{D}_{22}$ to region $\mathscr{D}_{23}$, then (1.46) undergoes a Hopf bifurcation, and a stable limit cycle bifurcates from $x = 0$.
(c) On the μ-parameter plane, if the point μ crosses the line l_3 from region $\mathscr{D}_{23}$ to region $\mathscr{D}_{21}$, then limit cycles of (1.46) undergo a fold bifurcation, i.e., the two limit cycles collide and then disappear.

1.9.5 Hopf–Hopf Bifurcation

The Hopf–Hopf bifurcation is a bifurcation of an equilibrium point in a two-parameter family of autonomous ODEs at which the critical equilibrium has two pairs of purely imaginary eigenvalues. This phenomenon is also called the double Hopf bifurcation. For example, consider the following two-parameter system:

$$\begin{aligned}
\dot{x}_1 &= \mu_1 x_1 - \omega_1 x_2 + (A_{11}x_1 - B_{11}x_2)(x_1^2 + x_2^2) + (A_{12}x_1 - B_{12}x_2)(x_3^2 + x_4^2),\\
\dot{x}_2 &= \omega_1 x_1 - \mu_1 x_2 + (A_{11}x_2 + B_{11}x_1)(x_1^2 + x_2^2) + (A_{12}x_2 + B_{12}x_1)(x_3^2 + x_4^2),\\
\dot{x}_3 &= \mu_2 x_3 - \omega_2 x_4 + (A_{21}x_3 - B_{21}x_4)(x_1^2 + x_2^2) + (A_{22}x_3 - B_{22}x_4)(x_3^2 + x_4^2),\\
\dot{x}_4 &= \omega_2 x_3 - \mu_2 x_4 + (A_{21}x_4 + B_{21}x_3)(x_1^2 + x_2^2) + (A_{22}x_4 + B_{22}x_3)(x_3^2 + x_4^2),
\end{aligned} \tag{1.50}$$

where $\sigma = \pm 1$, $\mu = (\mu_1, \mu_2) \in \mathbb{R}^2$, and $x = (x_1, x_2, x_3, x_4) \in \mathbb{R}^4$. At $\mu = 0$, the linearization of (1.50) at the equilibrium $(0,0,0,0)$ has two pairs of purely imaginary eigenvalues $\pm i\omega_1$ and $\pm i\omega_2$. Let $x_1 + ix_2 = \rho_1 e^{i\theta_1}$ and $x_3 + ix_4 = \rho_2 e^{i\theta_2}$. Then system (1.50) can be rewritten as

$$\begin{aligned}
\dot{\rho}_1 &= \rho_1(\mu_1 + A_{11}\rho_1^2 + A_{12}\rho_2^2),\\
\dot{\rho}_2 &= \rho_2(\mu_2 + A_{21}\rho_1^2 + A_{22}\rho_2^2),\\
\dot{\theta}_1 &= \omega_1 + B_{11}\rho_1^2 + B_{12}\rho_2^2,\\
\dot{\theta}_2 &= \omega_2 + B_{21}\rho_1^2 + B_{22}\rho_2^2.
\end{aligned} \tag{1.51}$$

Note that the amplitude and phase variables of (1.51) decouple. As a result, the bifurcation and asymptotic behavior of solutions of (1.50) can be studied via the following two-dimensional amplitude equations alone:

$$\begin{aligned}
\dot{\rho}_1 &= \rho_1(\mu_1 + A_{11}\rho_1^2 + A_{12}\rho_2^2),\\
\dot{\rho}_2 &= \rho_2(\mu_2 + A_{21}\rho_1^2 + A_{22}\rho_2^2).
\end{aligned} \tag{1.52}$$

The relation between equilibria of (1.52) and bifurcations of (1.50) is as follows:

(a) If (1.52) has an asymptotically stable (respectively, unstable) equilibrium $(r,0)$ (respectively, $(0,r)$) on either axis, then (1.50) has an asymptotically stable (respectively, unstable) periodic orbit of frequency close to ω_1 (respectively, ω_2).
(b) If (1.52) has an asymptotically stable (respectively, unstable) equilibrium (r_1,r_2) in the interior of the positive quadrant, then (1.50) has an asymptotically stable (respectively, unstable) two-dimensional invariant torus, i.e., (1.50) has a quasiperiodic solution in a neighborhood of the origin.
(c) If (1.52) has an asymptotically stable (respectively, unstable) limit cycle in the interior of the positive quadrant, then (1.50) has an asymptotically stable (respectively, unstable) three-dimensional invariant torus in a neighborhood of the origin.

From the above, we see that sufficiently close to the Hopf–Hopf bifurcation point $\mu = 0$, system (1.50) will exhibit either periodic or quasiperiodic motions. Thus, if we can find combinations of parameters μ_i and A_{ij} $(i,j = 1,2)$ that yield stable equilibria (r_1,r_2) with $r_1 r_2 \neq 0$, we can conclude that the stable quasiperiodic motions should occur for the corresponding parameter values of system (1.50). Therefore, from now on, we concentrate on describing the behavior of the coupled amplitude equation (1.52) in the μ-parameter plane. The mode interaction equations (1.52) have been investigated by many researchers. See, for example, Guckenheimer and Holmes [125, Sect. 7.5]. Here, for the sake of completeness, we shall employ some techniques from the above-mentioned classical work of Guckenheimer and Holmes (including rescaling in time and variables) to investigate the qualitative behavior of the mode interaction equations (1.52) in the parameter ranges of interest. We discuss these case by case.

First, we consider the case that $A_{11} < 0$ and $A_{22} < 0$. Introducing new phase variables according to

$$r_1 = \sqrt{|A_{11}|}\rho_1, \quad r_2 = \sqrt{|A_{22}|}\rho_2, \tag{1.53}$$

yields

$$\begin{aligned} \dot{r}_1 &= \mu_1 r_1 - r_1^3 - \theta r_1 r_2^2, \\ \dot{r}_2 &= \mu_2 r_2 - r_2^3 - \Delta r_2 r_1^2, \end{aligned} \tag{1.54}$$

where $\theta = A_{12}/A_{22}$ and $\Delta = A_{21}/A_{11}$. Notice that the r_1- and r_2-axes are invariant lines for the flow of (1.54). Simple linear analysis reveals the following results about equilibria of (1.54):

(a) $(r_1,r_2) = (0,0)$ is always an equilibrium. It is a stable sink if $\max\{\mu_1,\mu_2\} < 0$, a saddle if $\mu_1\mu_2 < 0$, and an unstable source if $\min\{\mu_1,\mu_2\} > 0$.
(b) $(r_1,r_2) = (\sqrt{\mu_1},0)$ is an equilibrium if $\mu_1 > 0$. If, in addition, $\Delta\mu_1 > \mu_2$, then it is a sink; otherwise, it is a saddle.
(c) $(r_1,r_2) = (0,\sqrt{\mu_2})$ is an equilibrium if $\mu_2 > 0$. If, in addition, $\theta\mu_2 > \mu_1$, then it is a sink; otherwise, it is a saddle.

(d) $(r_1, r_2) = (\sqrt{[\mu_1 - \theta\mu_2]/[1-\theta\Delta]}, \sqrt{[\mu_2 - \Delta\mu_1]/[1-\theta\Delta]})$ is an equilibrium if both radicands are positive. It is a saddle if $\theta\Delta > 1$ and a sink if $\theta\Delta < 1$.

Therefore, we deduce that bifurcations to the pure modes $(\sqrt{\mu_1}, 0)$ and $(0, \sqrt{\mu_2})$ occur on the lines $\mu_1 = 0$ and $\mu_2 = 0$, whereas bifurcations to the mixed mode occur on the lines $\mu_1 = \theta\mu_2$ and $\mu_2 = \Delta\mu_1$ if they exist. In addition, we need check that no closed orbits (or limit cycles) can occur. Since the r_1- and r_2-axes are invariant, any such closed orbit would have to lie in the interior of the positive quadrant and must enclose at least one equilibrium with Poincaré index equal to 1.

If $\theta\Delta > 1$ and $\mu_1 - \theta\mu_2 < 0$ and $\mu_2 - \Delta\mu_1 < 0$, then system (1.54) has an equilibrium $(\tilde{r}_1, \tilde{r}_2)$ with $\tilde{r}_1\tilde{r}_2 \neq 0$. Recall that $(\tilde{r}_1, \tilde{r}_2)$ is a saddle with Poincaré index equal to -1. We immediately see that no closed orbit can occur around $(\tilde{r}_1, \tilde{r}_2)$. If $\theta\Delta < 1$ and $\mu_1 - \theta\mu_2 > 0$ and $\mu_2 - \Delta\mu_1 > 0$, then system (1.54) has an equilibrium $(\tilde{r}_1, \tilde{r}_2)$ with $\tilde{r}_1\tilde{r}_2 \neq 0$, which is a sink. In what follows, we distinguish several cases to conclude that no closed orbits can occur around the sink $(\tilde{r}_1, \tilde{r}_2)$ when $\theta\Delta < 1$ and $\mu \in \mathscr{E} = \{\mu\colon \mu_1 - \theta\mu_2 > 0 \text{ and } \mu_2 - \Delta\mu_1 > 0\}$.

Case 1: $\theta > 0$ and $\Delta > 0$. We follow a directional arc $\overrightarrow{l_1}$ crossing the line $\mu_1 = \theta\mu_2 > 0$ and then passing through the sector $\mathscr{E}$ and finally crossing the line $\mu_2 = \Delta\mu_1 > 0$. When $\mu \in \overrightarrow{l_1}$ crosses the line $\mu_1 = \theta\mu_2 > 0$, the sink $(0, \sqrt{\mu_2})$ becomes a saddle, a sink $(\tilde{r}_1, \tilde{r}_2)$ bifurcates from $(0, \sqrt{\mu_2})$, and the unstable separatrix of the saddle $(0, \sqrt{\mu_2})$ limits this bifurcated sink $(\tilde{r}_1, \tilde{r}_2)$. Thus, after bifurcation there is no closed orbit around this sink. The only way whereby the closed orbit can appear in the positive quadrant is by Hopf bifurcation from $(\tilde{r}_1, \tilde{r}_2)$. But this is impossible, because $(\tilde{r}_1, \tilde{r}_2)$ remains stable for all $\mu \in \mathscr{E}$.

Case 2: $\theta > 0 > \Delta$. Similar arguments as those in Case 1 show that there is no closed orbit in the positive quadrant when μ is in the sector $0 < \mu_2 < \mu_1/\theta$. In order to rule out the existence of closed orbits in the positive quadrant when μ is in the sector $\Delta\mu_1 < \mu_2 < 0$, we follow another directional arc $\overrightarrow{l_2}$ crossing the line $\mu_2 = \Delta\mu_1$ and then passing through the sector $\Delta\mu_1 < \mu_2 < 0$. When $\mu \in \overrightarrow{l_2}$ crosses the line $\mu_2 = \Delta\mu_1$, the sink $(\sqrt{\mu_1}, 0)$ becomes a saddle, a sink $(\tilde{r}_1, \tilde{r}_2)$ bifurcates from $(\sqrt{\mu_1}, 0)$, and the unstable separatrix of the saddle $(\sqrt{\mu_1}, 0)$ limits this bifurcated sink $(\tilde{r}_1, \tilde{r}_2)$. Thus, after bifurcation there is no closed orbit around this sink. Similarly, no Hopf bifurcation can occur from $(\tilde{r}_1, \tilde{r}_2)$, since it remains stable for all $\mu \in \mathscr{E}$.

Case 3: $\theta < 0 < \Delta$. Similar arguments as those in Case 1 tell us that there is no closed orbit in the positive quadrant when μ is in the sector $\theta\mu_2 < \mu_1 < 0$, while arguments like those in Case 2 yield that there is no closed orbit in the positive quadrant when μ is in the sector $0 < \mu_1 < \mu_2/\Delta$.

Case 4: $\theta < 0$ and $\Delta < 0$. The discussion is similar to that in Case 1 and hence is omitted.

In summary, we have proved the following theorem.

Theorem 1.13. *No closed orbit of system (1.54) can occur around the mixed mode* $(\tilde{r}_1, \tilde{r}_2)$.

Second, for the case that $A_{11} > 0$ and $A_{22} > 0$, we introduce new phase variables and rescale time in (1.52) according to

$$r_1 = \sqrt{|A_{11}|}\rho_1, \quad r_2 = \sqrt{|A_{22}|}\rho_2, \quad t^* = -t. \tag{1.55}$$

After dropping $*$, we obtain

$$\begin{aligned} \dot{r}_1 &= -\mu_1 r_1 - r_1^3 - \theta r_1 r_2^2, \\ \dot{r}_2 &= -\mu_2 r_2 - r_2^3 - \Delta r_2 r_1^2, \end{aligned} \tag{1.56}$$

where θ and Δ are the same as before. System (1.56) is quite similar to (1.54), and hence similar arguments can be employed. We omit the details here.

Third, for the case that $A_{11} > 0$ and $A_{22} < 0$, we introduce new phase variables and rescale time in (1.52) as (1.53). After dropping $*$, we obtain

$$\begin{aligned} \dot{r}_1 &= \mu_1 r_1 + r_1^3 - \theta r_1 r_2^2, \\ \dot{r}_2 &= \mu_2 r_2 - r_2^3 + \Delta r_2 r_1^2, \end{aligned} \tag{1.57}$$

where θ and Δ are the same as before. Simple linear analysis produces the following results:

(a) $(r_1, r_2) = (0,0)$ is always an equilibrium. It is a stable sink if $\max\{\mu_1, \mu_2\} < 0$, a saddle if $\mu_1\mu_2 < 0$, and an unstable source if $\min\{\mu_1, \mu_2\} > 0$.
(b) $(r_1, r_2) = (\sqrt{-\mu_1}, 0)$ is an equilibrium if $\mu_1 < 0$. If, in addition, $\Delta\mu_1 < \mu_2$, then it is a source; otherwise, it is a saddle.
(c) $(r_1, r_2) = (0, \sqrt{\mu_2})$ is an equilibrium if $\mu_2 > 0$. If, in addition, $\theta\mu_2 > \mu_1$, then it is a sink; otherwise, it is a saddle.
(d) $(r_1, r_2) = (\sqrt{[\mu_1 - \theta\mu_2]/[\theta\Delta - 1]}, \sqrt{[\Delta\mu_1 - \mu_2]/[\theta\Delta - 1]})$ is an equilibrium if both radicands are positive. If $\theta\Delta < 1$, then it is a saddle; if $\theta\Delta > 1$ and $\tilde{r_1} > \tilde{r_2}$, then it is a source; if $\theta\Delta > 1$ and $\tilde{r_1} < \tilde{r_2}$, then it is a sink.

It follows from the above results that bifurcations to the pure modes $(\sqrt{-\mu_1}, 0)$ and $(0, \sqrt{\mu_2})$ occur on the lines $\mu_1 = 0$ and $\mu_2 = 0$, whereas bifurcations to the mixed modes occur on the lines $\mu_1 = \theta\mu_2$ and $\mu_2 = \Delta\mu_1$ if they exist. Since the r_1- and r_2-axes are invariant, any such closed orbit would have to lie in the interior of the positive quadrant and must enclose at least one equilibrium with Poincaré index equal to 1. If $\theta\Delta < 1$, $\mu_1 - \theta\mu_2 < 0$, and $\mu_2 - \Delta\mu_1 > 0$, then system (1.57) has an equilibrium $(\tilde{r}_1, \tilde{r}_2)$ with $\tilde{r}_1\tilde{r}_2 \neq 0$, which is a saddle with Poincaré index equal to -1. We immediately conclude the following result.

Theorem 1.14. *Assume that $\theta\Delta < 1$, $\mu_1 - \theta\mu_2 < 0$, and $\mu_2 - \Delta\mu_1 > 0$. Then no closed orbit of system (1.57) can occur around $(\tilde{r}_1, \tilde{r}_2)$.*

If $\theta\Delta > 1$, (μ_1, μ_2) is in the sector $\mathscr{S} = \{\mu\colon \mu_1 - \theta\mu_2 > 0, \text{ and } \mu_2 - \Delta\mu_1 < 0\}$, then system (1.57) has an equilibrium $(\tilde{r}_1, \tilde{r}_2)$ with $\tilde{r}_1\tilde{r}_2 \neq 0$. It follows from the expressions for $\tilde{r}_1$ and $\tilde{r}_2$ that $\text{sign}(\tilde{r}_1 - \tilde{r}_2) = \text{sign}(1-\theta)\text{sign}\{\mu_2 - \chi\mu_1\}$, where $\chi = (1-\Delta)/(\theta - 1)$. Furthermore, if $\theta > 1$, then $\chi < 1/\theta$ and $\chi < \Delta$; if $0 < \theta < 1$, then $\chi > 1/\theta$ and $\chi > \Delta$; if $\theta < 0$, then $\Delta < \chi < \frac{1}{\theta}$. Therefore, we have the following observations:

Lemma 1.4. *If $\Delta > 1/\theta > 0$ and $(\mu_1,\mu_2) \in \mathscr{I}$, then system (1.57) has a mixed mode $(\tilde{r}_1,\tilde{r}_2)$. Moreover, it is a sink (respectively, source) if μ is in the sector $\mathscr{I}_1$ (respectively, $\mathscr{I}_2$), where*

$$\mathscr{I}_1 = \begin{cases} \{\mu\text{: } \chi\mu_1 < \mu_2 < \mu_1/\theta\} & \text{if } \theta > 1, \\ \{\mu\text{: } \mu_2 < \chi\mu_1 \text{ and } \mu_2 < \mu_1/\theta\} & \text{if } \theta < 1, \end{cases}$$

$$\mathscr{I}_2 = \begin{cases} \{\mu\text{: } \mu_2 < \chi\mu_1 \text{ and } \mu_2 < \Delta\mu_1\} & \text{if } \theta > 1, \\ \{\mu\text{: } \chi\mu_1 < \mu_2 < \Delta\mu_1\} & \text{if } \theta < 1. \end{cases}$$

Lemma 1.5. *If $\Delta < 1/\theta < 0$ and $(\mu_1,\mu_2) \in \mathscr{I}$, then system (1.57) has a mixed mode $(\tilde{r}_1,\tilde{r}_2)$. Moreover, it is a sink (respectively, source) if μ is in the sector $\mathscr{I}_3$ (respectively, $\mathscr{I}_4$), where*

$$\mathscr{I}_3 = \{\mu\text{: } \mu_1/\theta < \mu_2 < \chi\mu_1\},$$
$$\mathscr{I}_4 = \{\mu\text{: } \chi\mu_1 < \mu_2 < \Delta\mu_1\}.$$

The following result describes the phase portrait of (1.57).

Theorem 1.15. *Assume $\theta\Delta > 1$. Then for some points $\mu \in \mathscr{I}$, system (1.57) has closed orbits surrounding the mixed mode $(\tilde{r}_1,\tilde{r}_2)$.*

Proof. Here, we consider only the case $\theta > 1 > \Delta > 1/\theta > 0$, because other cases can be handled similarly. If $\theta\Delta > 1$ and $\theta > 1$, then $\mu \in \mathscr{I}$ and system (1.57) has a mixed mode $(\tilde{r}_1,\tilde{r}_2)$. We follow a directional arc in the μ-parameter plane that starts from a point in the sector $\mu_1/\theta < \mu_2 < \Delta\mu_1$, then crosses the line $\mu_1 = \theta\mu_2 > 0$ into the sector $\mathscr{I}_1$, and finally successively crosses the line $\mu_2 = \chi\mu_1 > 0$ and the positive μ_1-axis. When the point μ is in the sector $\mu_1/\theta < \mu_2 < \Delta\mu_1$, system (1.57) has a source $(0,0)$ and a sink $(0,\sqrt{\mu_2})$. As μ crosses the line $\mu_1 = \theta\mu_2 > 0$, a mixed mode $(\tilde{r}_1,\tilde{r}_2)$ (which is a sink) bifurcates from $(0,\sqrt{\mu_2})$, and the unstable separatrix of the saddle $(0,\sqrt{\mu_2})$ limits the newly bifurcated mixed mode. Thus, immediately after bifurcation, no closed orbit can surround the mixed mode. However, as μ crosses the line $\mu_2 = \chi\mu_1 > 0$, the mixed mode $(\tilde{r}_1,\tilde{r}_2)$ loses its stability, and hence system (1.57) undergoes a Hopf bifurcation, i.e., a stable closed orbit appears in the positive quadrant. Moreover, as μ crosses the positive μ_1-axis, the pure mode $(0,\sqrt{\mu_2})$ collides with $(0,0)$ and disappears. □

Theorem 1.15 implies that crossing the line $\mu_2 = \chi\mu_1$ in the sector $\mathscr{I}$ results in the branching of a three-dimensional torus from the two-dimensional torus of system (1.52).

Finally, for the case $A_{11} < 0$ and $A_{22} > 0$, we can obtain the reparameterized equation of the form (1.57) by reversing time, and hence the details are omitted.

1.10 Some Other Bifurcations

1. *Nontransversal homoclinic orbit to a hyperbolic cycle*. Consider a three-dimensional system (1.1) with a hyperbolic limit cycle Γ_μ. Its stable and unstable two-dimensional invariant manifolds, $W^s(\Gamma_\mu)$ and $W^u(\Gamma_\mu)$, can intersect along homoclinic orbits, tending to Γ_μ as $t \to \pm\infty$. Generically, such an intersection is transversal. It implies the presence of an infinite number of saddle limit cycles near the homoclinic orbit. However, at a certain parameter value, say $\mu = \mu_0$, the manifolds can become tangent to each other and then no longer intersect. At $\mu = \mu_0$, there is a homoclinic orbit to Γ_0 along which the manifolds $W^s(\Gamma_\mu)$ and $W^u(\Gamma_\mu)$ generically have a quadratic tangency. It has been proved that an infinite number of limit cycles can exist for sufficiently small $|\mu - \mu_0|$, even if the manifolds do not intersect. Passing the critical parameter value is accompanied by an infinite number of period-doubling and fold bifurcations of limit cycles. See, for example, Poincaré [246], Birkhoff [34], Smale [268], Neimark [229], and Shil'nikov [263], Gavrilov and Shilnikov [110], Palis and Takens [243].
2. *Homoclinic orbits to a nonhyperbolic limit cycle*. Suppose a three-dimensional system (1.1) has at $\mu = \mu_0$ a nonhyperbolic limit cycle Γ_0 with a simple multiplier $\lambda_1 = 1$, while the second multiplier satisfies $|\lambda_2| < 1$. Under generic perturbations, this cycle Γ_0 will either disappear or split into two hyperbolic cycles (i.e., via fold bifurcation for cycles). However, the locally unstable manifold $W^u(\Gamma_0)$ of the cycle can *return* to the cycle Γ_0 at the critical parameter value $\mu = \mu_0$, forming a set composed of homoclinic orbits that approach Γ_0 as $t \to \pm\infty$. Thus, at the critical parameter value, there may exist a smooth invariant torus or a *strange* attracting invariant set that contains an infinite number of saddle and stable limit cycles, or a *blue-sky* catastrophe. See, for example, Afraimovich and Shil'nikov [4], Palis and Pugh [242], Medvedev [218], Turaev and Shil'nikov [279].
3. *Bifurcations on invariant tori*. Continuous-time dynamical systems with phase-space dimension $n > 2$ can have invariant tori. For example, a stable cycle in $\mathbb{R}^3$ can lose stability when a pair of complex-conjugate multipliers crosses the unit circle. It will be much more interesting to discuss changes of the orbit structure on an invariant 2-torus under variation of the parameters of the system. These bifurcations are responsible for such phenomena as frequency and phase locking. See, for example, Arnold [19], Fenichel [95, 96], Kuznetsov [200].